

THESIS FOR THE DEGREE OF DOCTOR OF PHILOSOPHY

Ab initio MODELLING OF ALKALI-ION
BATTERY ELECTROLYTE PROPERTIES

ERLENDUR JÓNSSON



CHALMERS

DEPARTMENT OF APPLIED PHYSICS
CHALMERS UNIVERSITY OF TECHNOLOGY
GÖTEBORG, SWEDEN
2014

***Ab initio* modelling of alkali-ion battery electrolyte properties**

ERLENDUR JÓNSSON

Göteborg, Sweden 2014

ISBN 978-91-7385-971-4

Doktorsavhandlingar vid Chalmers tekniska högskola

Ny serie nr: 3652

ISSN 0346-718X

Cover: Looking through a LiPF_6/EC electrolyte towards an anode

Department of Applied Physics

Chalmers University of Technology

SE-412 96 Göteborg, Sweden

© ERLENDUR JÓNSSON, 2014

Ab initio modelling of alkali-ion battery electrolyte properties

Erlendur Jónsson
Department of Applied Physics
Chalmers University of Technology
SE-412 96 Göteborg, Sweden

Abstract

Lithium-ion batteries are omnipresent in modern electronics. They can be found in laptops, mobile phones, and electric vehicles. However, there is room for both improvement, as the thermal instability of the dominant lithium salt used in batteries today, LiPF_6 , causes safety concerns, and more fundamental changes, as there is a limited amount of lithium available – resulting in sodium-ion batteries being a nascent field of study.

This thesis looks in detail at some underlying fundamental features affecting properties of electrolytes of both lithium-ion and sodium-ion batteries. These properties include the oxidative stability of the anions of the lithium and sodium salts (important for voltage and safety); the cation-anion interaction strength (important for conductivity); the solvation of the lithium and sodium cations in the common carbonate solvents (important for conductivity and the (de-)solvation at the anodes/cathodes); and the thermal stability of the anions and the possible decomposition reactions (important for safety).

The properties are mainly studied for a number of both novel and well established anions. Some of the novel anions involve completely new concepts for anion design for alkali-ion battery electrolytes.

The systems are studied with a number of *ab initio* methods, most based on density functional theory (DFT). These include high level calculations of benchmark quality. The applicability of DFT and the selection of DFT functionals is also studied. Novel calculation strategies were employed to understand thermal decomposition.

Keywords: Batteries, electrolytes, lithium salts, sodium salts, anions, *ab initio*, DFT

List of Publications

This thesis is based on the following publications

- I. **Novel lithium imides; effects of $-F$, $-CF_3$, and $-C\equiv N$ substituents on lithium battery salt stability and dissociation**
Johan Scheers, Erlendur Jónsson, Per Jacobsson and Patrik Johansson
Electrochemistry, 2012, **80** (1), 18-25
Electrochemistry, 2012, **80** (3), 142
- II. **Novel pseudo-delocalized anions for lithium battery electrolytes**
Erlendur Jónsson, Michel Armand and Patrik Johansson
Phys. Chem. Chem. Phys., 2012, **14** (17), 6021-6025
- III. **Modern battery electrolytes: Ion-ion interactions in Li^+/Na^+ conductors from *ab initio* calculations**
Erlendur Jónsson and Patrik Johansson
Phys. Chem. Chem. Phys., 2012, **14** (30), 10774-10779
- IV. **Solvation of Li^+ and Na^+ in cyclic and linear carbonate based battery electrolytes**
Erlendur Jónsson and Patrik Johansson
Submitted
- V. **Electrochemical oxidation stability of anions for modern battery electrolytes: A CBS and DFT study**
Erlendur Jónsson and Patrik Johansson
Submitted
- VI. **Thermal decomposition of ionic liquid based lithium-ion battery electrolytes – a combined *ab initio* and experimental study**
Erlendur Jónsson, Susanne Wilken and Patrik Johansson
Manuscript
- VII. **Spectroscopic and computational study of cation solvation in lithium-ion and sodium-ion battery electrolytes**
Erlendur Jónsson, Luis Aguilera, Damien Monti, Aleksandar Matic and Patrik Johansson
Manuscript

Additional publications not included in the thesis

VIII. Anions and derived salts with high dissociation in non-protogenic solvents

Erlendur Jónsson, Michel Armand and Patrik Johansson

U.S. Provisional Patent Application, Serial No. 61/560,942

Filing Date: November 17, 2011

International Patent Application No. PCT/EP2012/072858

Filing Date: November 16, 2012

IX. Solvate structures and computational/spectroscopic characterization of lithium difluoro(oxalato)borate (LiDFOB) electrolytes

Sang-Don Han, Joshua L. Allen, Erlendur Jónsson, Patrik Johansson,

Dennis W. McOwen, Paul D. Boyle and Wesley A. Henderson

J. Phys. Chem. C, 2013, **117** (11), 5521-5531

X. Ionic liquid based electrolytes for sodium-ion batteries: Na⁺ solvation and ionic conductivity

Damien Monti, Erlendur Jónsson, M. Rosa Palacín and

Patrik Johansson

J. Power Sources, 2014, **245**, 630-636

Contribution Report

Paper I I designed, together with JS, the thermal stability calculation methodology. I did all of the bond breaking calculations. I took minor part in writing the manuscript.

Paper II I did all of the calculations for the article, analysed the results and wrote the main part of the manuscript. The concept was founded by MA, but I designed the pd-index.

Paper III Me and PJ designed the study. I did the all of the calculations, analysed the results and wrote the main part of the manuscript.

Paper IV I did all of the calculations, analysed the results and wrote the main part of the manuscript.

Paper V I designed the study, did the calculations, analysed the results and wrote the main part of the manuscript.

Paper VI I programmed the decomposition program (Appendix A), performed the calculations, analysed the *ab initio* results and wrote the main part of the manuscript together with SW.

Paper VII Me and PJ designed the study. I performed the calculations, analysed the *ab initio* results and wrote the main part of the manuscript together with LA.

List of Acronyms

CC	Coupled cluster
CBS	Complete basis set
CI	Configuration interaction
DFT	Density functional theory
DMC	Dimethyl carbonate
EA	Electron affinity
EC	Ethylene carbonate
ESW	Electrochemical stability window
EV	Electric vehicle
GGA	General gradient approximation
HF	Hartree-Fock
IL	Ionic liquid
IP	Ionisation potential
LIB	Lithium-ion battery
LSDA	Local spin-density approximation
QC	Quantum chemistry
RTIL	Room temperature ionic liquid
SCF	Self consistent field
SEI	Solid electrolyte interphase
SIB	Sodium-ion battery

For a comprehensive list of anion acronyms, see appendix B.

Contents

Abstract	i
List of Publications	iii
Contribution Report	v
List of Acronyms	vi
List of Figures	ix
1 Introduction	1
2 Batteries	3
2.1 Lithium-ion batteries	5
2.1.1 Anodes	6
2.1.2 Cathodes	7
2.2 Electrolytes	7
2.2.1 Salts	9
2.2.2 Solvents	13
2.2.3 Additives	14
2.2.4 Ionic liquids	14
2.3 Sodium-ion batteries	15
2.4 Impact of <i>ab initio</i> calculations	16
3 Techniques	19
3.1 The Schrödinger equation	19
3.2 Basis sets	20
3.2.1 CBS limit	22
3.3 Wave-function methods	22
3.3.1 Hartree-Fock, 2nd order Møller-Plesset and Configuration Interaction	23
3.3.2 Coupled Cluster	25

3.4	Density Functional Theory	26
3.4.1	Functionals	26
3.4.2	Hardness and softness	29
3.5	CBS methods	29
3.5.1	Composite methods	30
3.5.2	Approximate CBS	30
3.6	Atoms in molecules	31
3.7	Derivatives	31
3.7.1	Optimisation	31
3.7.2	Spectra	32
4	Applications and Results	33
4.1	Ion-pair dissociation energy	33
4.2	Solvation energy	35
4.3	Oxidation potential	37
4.4	Thermal stability	40
4.4.1	Bond breaking and recombination	41
4.5	Localization	42
5	Summary of Appended Papers	43
6	Conclusion and Outlook	47
	Acknowledgements	49
	Bibliography	51
	Appendices	67
A	Recombinator program	67
B	Anions	69

List of Figures

1	The early Daniell's cell	4
2	A schematic depiction of a LIB's charge cycle	5
3	A sketch of a modern battery with its components	6
4	Common anions used in lithium-ion batteries	10
5	Common solvents used in lithium-ion batteries	13
6	The EMIm cation	14
7	Na ⁺ intercalation in hard carbons	15
8	SCF loop illustrated	20
9	The overlap, $\phi_i * \phi_j$, of two different gaussian functions, ϕ_i and ϕ_j , is a gaussian	21
10	Contour of the electron density of HF	23
11	The cluster operator $\hat{T} = \hat{T}_1 + \hat{T}_2$ acting on a two electron system	25
12	Local minima vs. a global minimum	32
13	The making of charge carriers	34
14	The ion-pairs of NaBOB	35
15	The Frank-Condon approximation and the true ionisation potential	38
16	A Scheers plot of the pseudo-delocalized anions	39
17	A demonstration of the bond breaking strategy	41
18	A number of imides, where R ₁ and R ₂ can be one of -F, -CF ₃ and -C≡N.	43
19	A schematic drawing of the pseudo-delocalized anion concept	44
20	$\Delta E_{d Li}$ vs. $\Delta E_{d Na}$	45

Chapter 1

Introduction

Batteries, those storage units of electrochemical energy, are key components of modern technology. They are used for many purposes, such as providing primary and backup power for computers, powering medical implants and mobile electronics. The lithium-ion battery (LIB) holds a special place amongst the rechargeable batteries due to its versatility for mobile applications.¹

Many popular portable electronics, such as laptops, many an iDevice, and some power tools, have one form or another of a LIB. There is an ever increasing demand of higher and higher capacity batteries, both for the growing smartphone market and the nascent electric vehicle (EV) market. Especially now following the success of the Tesla EVs – the most sold car in Norway in September 2013...²

The application of batteries is common in smaller applications, but not limited to them. Large-scale industrial applications include the augmentation of electrical grids, to load-level the electrical production of certain sustainable power plants, such as solar and wind power plants.³ Thus using solar power at night would be a possibility (albeit indirect).

Thus, there is a considerable interest in the production of LIBs, and also in reducing their environmental impact. Despite being a critical component for green technology, they are not particularly green themselves, though that is dependent on their chemistry. LIBs are a key component of technology that is aimed at a consumer audience, thus making their increased safety paramount. Especially following spectacular failures of such batteries. Other issues include cyclability of the batteries, *i.e.* their lifetime, the material costs and the capacity of the battery.

Both the material costs and the environment are impacted by the limited availability of lithium, which (when coupled with the rapidly increasing demand for it) is driving up prices for Li_2CO_3 on commodity markets,⁴

which has even prompted comparisons with gold.⁵ Thus, batteries with alternate chemistries that can either supplant or supplement LIBs would be of immense benefit. One key possibility is sodium-ion batteries (SIB) – recently popularised in research. SIBs would not have the same resource constraints as LIBs due to the vast availability of sodium (both on the market and as raw natural resources). However, graphite is not an option for the SIB anode due to the the difference in intercalation chemistry⁶ – though novel materials might remove that issue entirely.⁷

Some of the issues of LIB can in part be sourced to the electrolyte (though not all⁸), which is composed of aprotic solvent(s), functional additives and at least one salt. In the case of commonly available LIBs, the solvent is a mixture of ethylene and dimethyl carbonate (EC and DMC) and the salt is lithium hexafluorophosphate, LiPF_6 . This salt has the problem that when it decomposes, *e.g.* in a fire, the resulting fumes that are evolved tend to be quite poisonous, a hazard in addition to the flammability of organic solvents. Additionally, fluorine chemistry is tricky and therefore always expensive.

The development of new electrolytes, addressing both the problems of stability and resources, must be approached on the interdisciplinary border of material science, physics and chemistry. One of the available tools for that development is the modelling.

Typically, such modelling could include *in silico* synthesis of novel electrolyte salts or a thorough study of the cation-solvent interaction. The latter is a intensely debated topic in battery research as the exact role and extent of these interactions, in bulk and at the interfaces, is not yet fully known. Other electrolyte aspects that need to be understood for a rational selection to occur, include their thermal stability and possible decomposition products, and their electrochemical stability windows (ESW), *i.e.* their tolerance towards redox reactions.

This thesis is a computational study of some the issues of the electrolyte that are raised in this introduction, *i.e.* the study of novel lithium salts, sodium salts for SIBs, thermal stability and ESWs of salts, and studies of the cation-solvent interaction. In addition, a large number of theoretical techniques are described briefly, as they are used in the research on these topics.

Chapter 2

Batteries

Batteries are electrochemical devices, *i.e.* they store energy in chemical form and can release it as electricity. One early such device is the Daniell's cell*, as seen in Figure 1. It is also the first battery to employ, in 1838, a porous membrane to control the flow of ions.⁹

The basic components of batteries, now ≈ 170 years later, are still the same; electrodes (*i.e.* an anode and a cathode), an electrolyte and a separator. The cathode[†] is the positive electrode as electrons flow to them to reduce atoms/molecules. The anode, where there is an excess of electrons generated (*ergo* a negative charge), something must oxidise.

Battery performance can be characterised by quite a few parameters. Some examples include the battery's voltage (V) which depends on the relative potentials of the two chemical species participating in the redox reactions at the electrodes, and two other related parameters are the battery's power (W kg^{-1}) and gravimetric energy density (Wh kg^{-1}).¹⁰ These parameters are not independent of each other – the voltage determines in part the power density, as $\text{power} = \text{voltage} * \text{current}$.

Batteries are usually split into two categories, primary and secondary batteries. Primary batteries (which tend to be assembled fully charged) are used until the depletion of their energy and are subsequently discarded, hopefully to be recycled. These include for example alkaline batteries found in most convenience stores.

Secondary batteries can be recharged, *i.e.* after the depletion of their charge. These batteries are essentially omnipresent in modern society. They include old technologies like the lead-acid batteries found in cars and the

*There have been fascinating speculations that the first battery was actually created in Baghdad, nearly 1500 years before the discovery of electricity.

[†]Formally this gets reversed on charging, but to simplify things, electrodes are referred to their discharged state in the battery literature.

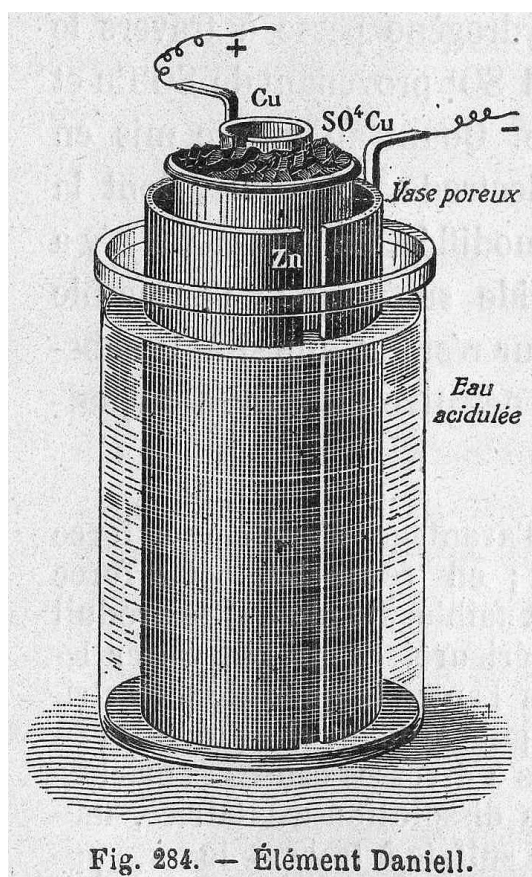


Figure 1: The early Daniell's cell which has a copper cathode in a CuSO_4 solution and a zinc anode in a ZnSO_4 solution. A porous ceramic material is used to separate the two half-cells. From *Leçons de Physique*; Éditions Vuibert et Nony by Gillard (in public domain via the Wikimedia Commons).

more modern such as LIBs used in a large number of mobile electronics applications.

On the horizon new battery chemistries have been proposed, such as aluminium-ion¹¹ and magnesium-ion batteries.¹² However, these novel systems are still under development and commercialisation of these systems is most likely in the far distant future. SIBs are another system that is under development, however, this is far closer to commercialisation as evidenced by being proposed for specific applications, such as stationary storage.¹³

LIBs and SIBs are the foci of the research in this thesis – more specifically, the common focus is on the properties of their electrolytes. However, some general information about the electrodes is also given, to be able to understand the integral role of the electrolyte.

2.1 Lithium-ion batteries

Lithium is an attractive material for batteries due to its low weight, low density and its high standard electrode potential of -3.04 V versus the standard hydrogen electrode.¹⁴ Li also has a small radius, thus it is easy to intercalate into electrodes. The first lithium batteries were primary batteries that found use in high-capacity applications.¹

The subsequent development of lithium secondary batteries was not without problems. During the charge-discharge cycle, an uneven distribution of deposited lithium caused dendrite formation on the lithium metal surface,¹⁵ which could short-circuit and in some cases start fires. To counteract this problem, the lithium metal was replaced with an intercalating material (more details in the anode and cathode chapters of the thesis).¹⁶

The secondary batteries that replaced the lithium metal batteries are now known as lithium-ion batteries. Sony commercialised these batteries in the 1990's.¹⁷ During their development, other terms were proposed for them such as rocking-chair¹⁸ and shuttlecock¹⁶ batteries. All of these terms are derived from the battery behaviour where lithium ions are transferred between the intercalation electrodes (Figure 2).

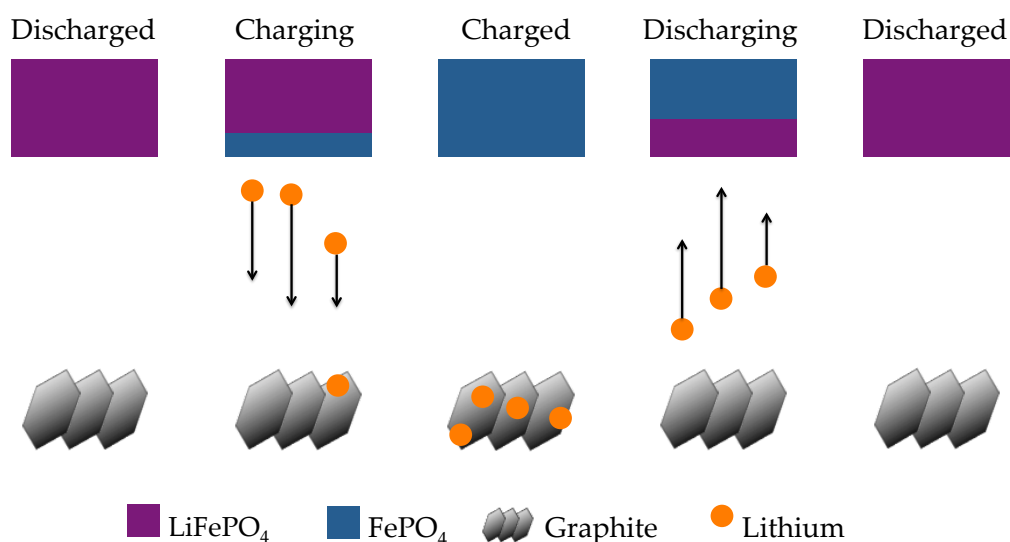


Figure 2: A schematic depiction of a LIB's charge cycle. During charging Li^+ ions get transported from the LiFePO_4 cathode over to the anode, where they get reduced into Li and intercalated into the graphite.

The modern LIB has a large number of components, which include the anode, cathode and electrolyte (Figure 3) and the more esoteric additives¹⁹

such as redox shuttles²⁰⁻²² and SEI formers.²³ While this thesis focuses exclusively on the electrolyte of these batteries, some basic understanding of the two other major components is needed.

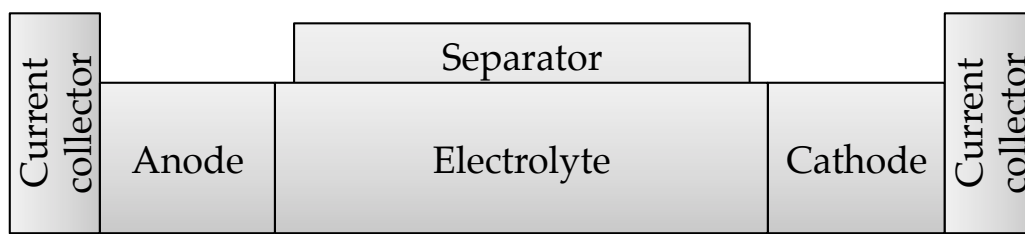


Figure 3: A sketch of modern battery with its components: the current collectors on both anode and cathode, the electrolyte that conducts ions between electrodes, and a separator that allows ion conduction but prevents a short circuit.

As Figure 2 shows, during discharge a LIB has lithium cations flowing from the anode to the cathode. The oxidation reaction of lithium ($\text{Li} \rightarrow \text{Li}^+ + e^-$) taking place at the anode forces electrons to do work by flowing through an electrical circuit. The opposite happens during charging, where an externally applied current forces the lithium to move from the cathode to the anode.

Note that a physical separator is needed in between the two electrodes, *e.g.* a membrane that is semi-permeable (it must allow the transport of Li^+ between the electrodes). For further information, see the comprehensive review by Arora and Zhang.²⁴

As the field of batteries is vast,^{25,26} this thesis will not go into all the details of a modern working battery (it will *e.g.* ignore organic electrodes). Thus for further information see for example recent reviews by Marom *et al.*²⁷ or Palacín.¹⁰ Recent books are available, such as Huggins' monograph²⁸ or the handbook edited by Daniel and Besenhard.²⁹

2.1.1 Anodes

The original lithium metal anodes were laden with safety issues, due to their tendency to form dendrites upon cycling. These dendrites can cause short-circuits, which may end in a fire.¹ By replacing the lithium metal with a carbonaceous structure, originally pyrolytic carbon,³⁰ but now replaced by graphite or graphite-like carbon structures,¹⁷ which then is intercalated with lithium ions, the safety increased considerably. Furthermore, the usage

of graphite as anode only reduces the operating voltage of the full cell by 0-0.3 V vs. Li^+/Li^0 ¹⁶ – making it a good choice for the anode.

Interestingly, it was discovered that the electrolyte reacts with the surface of the graphite anode, resulting in a thin protective layer that was dubbed solid electrolyte interphase (SEI).³¹ The SEI conducts ions, but is electrically insulating and its properties are highly dependent on the electrolyte composition.^{32,33} Numerous studies have been done on the exact reactions that create the SEI, both experimental and theoretical.³⁴⁻⁴⁴

Another popular anode material, despite its high insertion voltage, ≈ 1.5 V vs. Li^+/Li^0 , is lithium titanate,⁴⁵ $\text{Li}_4\text{Ti}_5\text{O}_{12}$. For some applications, the advantage of having excellent cyclability and fast insertion/deinsertion of Li^+ outweighs the voltage and concomitant energy density drop.

2.1.2 Cathodes

The cathode needs, like the anode, to be able to store lithium without deformation (otherwise the expansion/contraction can threaten the battery's physical integrity) and needs to be stable at high voltages. For the mass adoption of a new material preferably also environmentally benign and cheap.⁴⁶

The cathodes of the LIBs tend to be made of transition metal compounds, LiTiS_2 ⁴⁷ is an early example. However, it was found that LiCoO_2 was superior⁴⁸ and therefore subsequently used in the first commercial lithium-ion batteries.¹⁷ Another transition metal oxide used as a cathode is the lithium manganese spinel, LiMn_2O_4 .⁴⁹

An important development has been the discovery of LiFePO_4 as a viable cathode material. While it does not have as high energy density as LiCoO_2 , it is both more environmentally friendly and less expensive.⁵⁰ It also gives an insight into the financial and legal side of LIB research.⁵¹ A variation on the phosphates are the fluorophosphates, with the first being LiVPO_4F .⁵² Novel cathode materials are proposed for higher density, *i.e.* energy density, and the need for more power,⁵³ *i.e.* rate capability and high voltages.⁵⁴⁻⁵⁶

For a review on both the history of the cathode materials and how their structures affect their functionality, see Whittingham.⁴⁶

2.2 Electrolytes

Electrolytes mediate the transfer of lithium ions between the electrodes, thus balancing the charge transfer. Therefore electrolytes play a key role in

the conductivity inside batteries (the detailed picture is nuanced as seen in the review by Park *et al.*⁵⁷). As noted in the Introduction, the electrolyte of a LIB is typically made of a lithium salt, such as LiPF_6 , and a solvent mixture of *e.g.* ethylene carbonate (EC) and dimethyl carbonate (DMC). The current battery technology puts high demands, especially electrochemically, on the electrolyte, which must be stable in order to not degrade battery performance and/or safety.

As the role of the electrolyte is to transfer ions between the electrodes, it must allow for good ion conduction, *i.e.* high conductivity. For practical applications, the conductivity should be on the order of 1-10 mS/cm.⁵⁸ To allow for such high values, these electrolytes tend to be liquids. However, polymer electrolytes are also used and researched (see Ref.⁵⁹ and references therein). Such polymer electrolytes tend to have lower conductivities, on the order of 10^{-5} S/cm.⁶⁰ A difference of 2-3 orders of magnitudes in conductivity, however, can in part be compensated for by using a thin-film electrolyte.⁵⁹

The conductivity of a liquid electrolyte depends on a number of factors, including macroscopic factors such as its fluidity/viscosity, and its liquid range and microscopic factors such the nature of the charge carrying species and their behaviour in the electrolyte. In this thesis the charge carrying species are studied in detail, both to understand the cation-anion interaction and the solvent-cation interaction. As fluidity is a macroscopic property which not easily connected to molecular interactions, it is not studied in this thesis.

The stability of the electrolyte is another important property, both electrochemical and thermal. The electrochemical stability is characterised by the ESW, *i.e.* the difference between the voltages of oxidation and reduction reactions of the electrolyte. The reduction limit is set by the solvent and the electrode, as the reduction of the electrolyte anions is rare.⁶¹⁻⁶³ The oxidation limit of the electrolyte is set by the anion of the electrolyte salt. These limits are set by their properties, such as the HOMO/LUMO gap of the electrolyte and the band gap between the valence and conduction band of the electrodes²⁶ – ignoring stabilisation due to external effects, such as the formation of a SEI layer. Furthermore, this emphasises a thermodynamic approach which can differ from the real system due to kinetics. The oxidation limit, *i.e.* the oxidation potential, is studied in this thesis, both using established techniques⁶⁴ and novel approaches (Paper V).

The thermal stability of the electrolyte depends on the salt as the solvent is usually far more stable with respect to temperature (even have clear boiling points). Thus each salt must studied with respect to their thermal

stability, *e.g.* with thermogravimetric analysis (TGA), which has shown that LiPF_6 decomposes at 200°C , while LiBOB does so at 300°C .⁶⁵ However, these values are not representative for the thermal stability of the complete electrolyte system as LiPF_6 has been shown to decompose in EC/DMC at 85°C .⁶⁶ The thermal stability and decomposition is touched upon in Paper I and Paper VI.

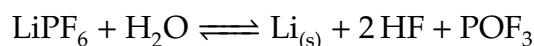
The battery components chemical compatibility/stability with respect to each other is another factor. Thus a new component must either be compatible with the current components of the battery, *e.g.* the current collectors, or new components must be developed, which is a non-trivial proposition. Other factors that are used for the rational selection of electrolyte components, include the toxicity,⁶⁷ environmental impact and cost.

In depth reviews are available for the electrolytes, such as the seminal review by Xu⁶⁸ and the book chapter by Gores *et al.*⁵⁸ Xu and von Cresce's review on the interface between electrolytes and electrodes⁶⁹ is also recommended.

2.2.1 Salts

Due to the demanding environment, the selection of a lithium salt must be made with all due care. An ideal lithium salt must be electrochemically stable, not react with any parts of the battery (except if it is beneficial for the battery), must dissociate (almost) completely into conducting cations and anions to ensure a high conductivity, must be environmentally friendly, cheap to mass produce, and easy to handle. However, no single salt qualifies for all these conditions.⁶⁸ Common salts (seen in Figure 4) include: LiTFSI (lithium bis(trifluoromethylsulfonyl) imide), which, however, corrodes the aluminium current collectors commonly used.⁷⁰ LiAsF_6 is a toxic carcinogen, while LiClO_4 is a very reactive strong oxidant. LiBOB (lithium bis(oxolato) borate) is electrochemically stable and non-toxic,⁷¹ but has a combination of "low solubility" (ranging from 0.8 M to 1 M in EC/DMC mixtures^{72,73}) and low conductivity^{72,74} (only half of LiPF_6 ⁷⁵).

LiPF_6 , the most common salt in usage today, is a compromise of the aforementioned factors. It has a high electrochemical stability (≈ 6.8 V vs. Li^+/Li ⁰⁷⁶) and conductivity (10.7 mS/cm in 1 M LiPF_6 in EC/DMC⁷⁷). However, it is thermally sensitive and in the presence of moisture it decomposes into poisonous compounds:⁶⁸



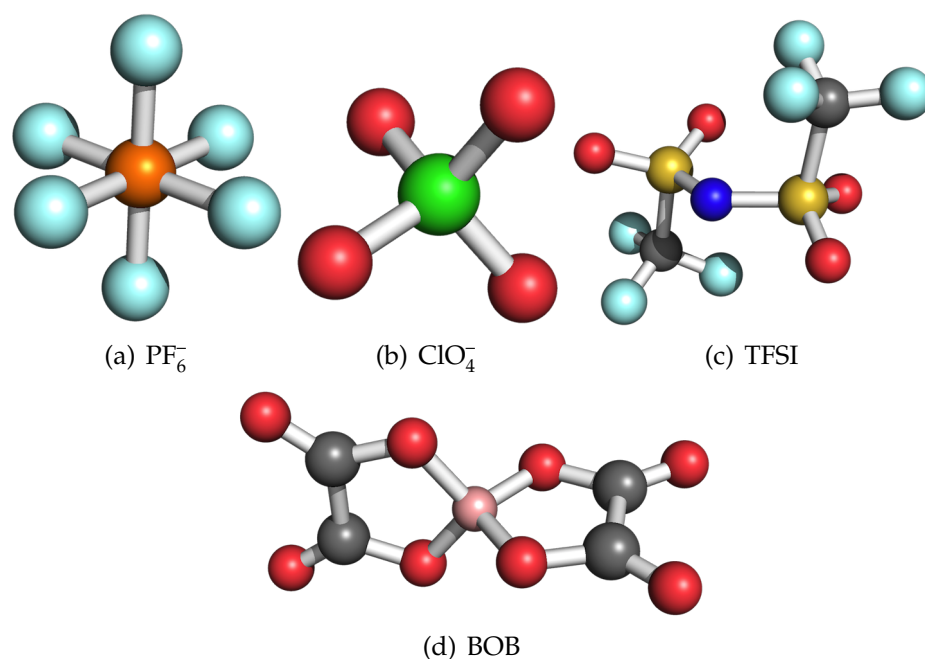
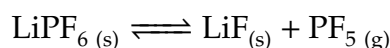
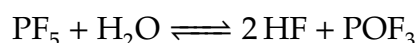


Figure 4: Common anions studied as lithium salts in electrolytes.

Furthermore, PF_5 exists in equilibrium with LiPF_6 :



There is also a decomposition reaction of PF_5 in the presence of moisture:



This set of degradation mechanisms has been studied in detail by several groups; see ref. 78 and references therein.

There is a large number of anions that have been proposed for LIB electrolytes[‡], as there is an interest to replace PF_6^- due to its the flaws mentioned earlier and that other anions may have properties which provide more benefits, *e.g.* better SEI formation, and lower cost due to a lack of fluorine in the molecule. However, fluorine is a very common element in the design of these anions due its high electronegativity, which allows for a delocalization of the anion's charge, which allows for a higher oxidation potential.^{79,80} Eight, somewhat arbitrarily defined, groups of anions are:^{81,82}

- SIMPLE ANIONS include elemental anions, such as F^- and Cl^- , and common anions such as acetate, CH_3COO^- , and nitrate, NO_3^- .

[‡]A comprehensive list of these anions can be found in Appendix B.

- TRADITIONAL WEAKLY COORDINATING ANIONS with PF_6^- as the most prominent example and including also perchlorate, ClO_4^- , triflate, CF_3SO_3^- , and hexafluoroarsenate, AsF_6^- .
- IMIDE ANIONS are based on NSO_2 chemistry, *e.g.* the triflate group (CF_3SO_2^-), which is used in the TFSI anion. FSI (bis(fluorosulfonyl) imide) is a shortened version of TFSI, initially found to be corrosive⁸³ towards the Al current collector, later shown by Han *et al.*⁸⁴ to be due to Cl^- impurities rather than a limitation of the FSI anion itself. Asymmetrical imides, such as FTFSI,⁸⁵ the intermediate structure between FSI and TFSI, also exist. Additionally, cyanosulfonyl groups $\text{N}\equiv\text{CSO}_2^-$, thus CSI, CFSI, *etc.*, have been explored⁸⁵ as have the use of a phosphoryl group, *e.g.* bis(dicyanophosphoryl) imide, CPI. There are also two cyclic imides reported by Murmann *et al.*⁸⁶
- BORON BASED ANIONS[§] can be split roughly into two groups. The aromatic structures were described in a series of papers by Barthel, Gores and others.^{79,87-91} This group also includes a number of salicylato-borate⁸⁹ derivatives, which have recently been reported to act also as additives.⁹² The non aromatic borates include a bis(perfluoropinacolato)orthoborate (BPFPB),⁹³ one of the most fluorinated anions reported in the battery literature[¶]. BPFPB is, however, a very impractical molecule, due to the 24 F atoms! Xu and Angell also reported BOB ($[\text{B}(\text{C}_2\text{O}_4)_2]^-$) (and also bis(malonato)borate (BMB, $[\text{B}(\text{C}_3\text{H}_2\text{O}_4)_2]^-$)).⁷¹ BOB is popular, due to the high thermal stability and good SEI formation.⁷² It also stabilises the graphite anode against PC, thus reducing/stopping exfoliation.⁹⁴ Yamaguchi *et al.* introduced perhalogenated carboxylic borate esters.⁹⁵ Breaking the symmetry of the borates gave rise to the BOB/BMB hybrid, (malonatooxalato)borate, MOB.⁹⁶ Another asymmetrical borate, the difluoro(oxalato)borate (DFOB),⁶⁵ has proved promising due its higher conductivity than BOB⁹⁷ yet similar SEI formation properties.⁹⁸
- PHOSPHORUS BASED ANIONS can partly be described as PF_6^- derivatives, such as PF_5CF_3^- ,⁹⁹ *etc.* Others can be described as phosphorus analogues of the borates, such as tris(oxalato)phosphate,¹⁰⁰ TOP analogous to BOB. The same holds for P1,¹⁰¹ P2, P3 and BBB, F-BBB and 4F-BBB. There is even a TFOP (comparable with DFOB),¹⁰² though it

[§]Note: BF_4^- and its derivatives are in the traditional weakly coordinating group.

[¶]Its name is also the closest to the name of a cocktail (piña colada) in the battery literature.

was serendipitously discovered as a reaction product from PF_6^- with BOB.¹⁰³

- HETEROCYCLIC BASED ANIONS include the Hückel type anions, such as TADC (N_5C_4^-)¹⁰⁴ and others that conform to the $\text{N}_5\text{C}_{2n}^-$ ($n = 0, \dots, 5$) formula. A few di-cyano-imidazole derivatives with perfluorinated alkyl groups have also been reported.¹⁰⁵⁻¹⁰⁷ Imidazole was also the basis for a number of anions that have BF_3 in a Lewis acid-base complex.^{108,109}
- PSEUDO-DELOCALIZED ANIONS are a group of anions that have two negative moieties and one positive, thus a formal charge of -1, discussed in detail in Paper II.⁸² They come in many different forms, due to the freedom in selection of the electronegative functional groups and the cationic core, but are yet to be electrochemically characterised.
- OTHERS are the anions the did not fit in with the rest, such as for example $\text{Al}(\text{HFIP})_4^-$.¹¹⁰

Looking over this large number of anions (and those in the appendix), some general comments are in order. New structural themes are introduced intermittently. These novel themes then undergo an evolution, where functional groups are exchanged for other groups, often more electronegative ones. An example is the fluoroalkylphosphate⁷⁷ (FAP, $[\text{P}(\text{C}_2\text{F}_5)_3\text{F}_3]^-$). This anion is similar to PF_6^- but where fluorine atoms have been exchanged for even more fluorine in the form of perfluorinated alkyl chains.

Another example is the bis(croconato) borate¹¹¹ (BCB, $[\text{B}(\text{C}_5\text{O}_5)_2]^-$). It is similar to both BOB and BMB, as the two H in the structure of the malonato moiety have been replaced by a double bonded oxygen atom. This removal of hydrogen increases the oxidative stability from ≈ 4.5 V for BMB to 5.5 V vs. Li^+/Li^0 for BCB.

Symmetry breaking is another theme recurring in the anion evolution. Thus PF_5CF_3^- and PF_5CN^- are similar to PF_6^- . The same goes for DFOB and BOB (and their phosphorus analogues, TFOP and TOP). Systematic studies often include these kind of asymmetries, such as the BF_3CN^- and $\text{BF}(\text{CN})_3^-$ anions¹¹² and the imide series of Scheers *et al.*⁸⁵ This strategy allows for some tuning of the electrolyte properties, as the properties can be an average of the two symmetric structures. The asymmetry can also increase the conductivity and the solubility.⁵⁸

Another trend that has appeared is the utilisation of multipurpose anions. They can form charge carriers, protect the anode from PC^{94} and can also function as additives, such as the salicylato borates.⁹²

2.2.2 Solvents

Another crucial aspect of electrolyte design is the solvent (a selection is seen in Figure 5). Propylene carbonate (PC) was the solvent of choice for the first commercialised batteries.¹⁷ This choice proved unfortunate as PC was found to damage the carbon anode as it got intercalated into the anode and decomposed into gases, thus exfoliating the anode.³²

Thus another solvent was to be used, *i.e.* ethylene carbonate (EC), which protects the carbon anode.³³ In hindsight, the simple methyl group in PC, compared with EC, slowed down the development of lithium batteries possibly by four decades.⁶⁹

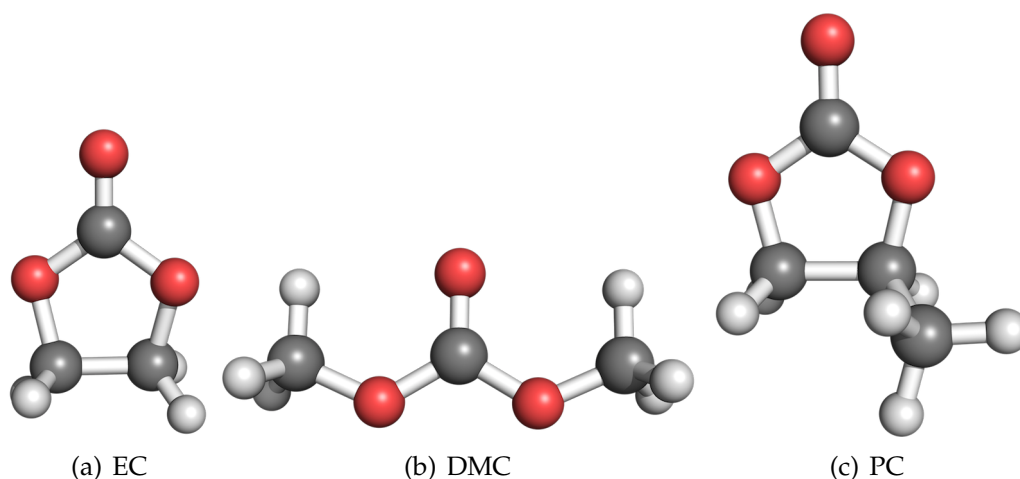


Figure 5: Common solvents used in LIBs.

As EC is a solid at room temperature, another carbonate solvent, dimethyl carbonate (DMC), is used with EC to bring down the melting point.⁶⁸ Interestingly, there is an on-going debate of the exact role of DMC in the electrolyte, some show that DMC plays no active role,^{113–115} while others show DMC to directly participate in the solvation of the lithium cation.^{35,116–118} This is despite the large number of experimental techniques used, including IR/Raman^{115–117} NMR^{119–121} and MS.^{113,114} *Ab initio* studies also have diverging conclusions, however, they also give an insight to the underlying issue. The differing results of MD simulations of Borodin and Smith¹¹⁸ and Postupna *et al.*¹²² show on different assumptions. Assuming a static DMC, it will not participate in the solvation of Li^+ , while it will solvate Li^+ if you allow for conformational flexibility. This is further explored in Paper IV.

While carbonate solvents are very common in the field of LIBs, other concepts are present *e.g.* silicon based solvents, shown to stabilise the PF_6^-

anion thermally.¹²³ Another is sulfone solvents, promising for high voltage cathodes.¹²⁴

2.2.3 Additives

To tailor the properties of the electrolytes, additives can be used for a number of purposes. Typical additives are vinyl carbonate^{125,126} used to improve the formation of the SEI layer and thus increasing the battery performance, and redox shuttles, which enable overcharge protection,²⁰⁻²² and the improvement of cycle life.¹²⁷ For further information, the review by Zhang²³ or the recent book chapter by Wilken *et al.*¹⁹ are recommended.

2.2.4 Ionic liquids

Ionic liquids (ILs) are salts with a melting point of 100°C or less, and those mainly studied are liquids at room temperature (RTIL). They are usually comprised of a bulky cation and an anion, for example 1-ethyl-3-methylimidazolium TFSI (EMIm is seen in Figure 6). As both ions can be varied extensively, ILs are often referred to as designer solvents.^{128,129} They often are non-flammable (especially with their low vapour pressure), non-toxic and easy to handle. They also tend to be electrochemically stable. Their thermostability is studied in Paper VI.

Due to these reasons, ILs have been explored as electrolyte matrices for LIBs.¹³⁰ A Li-salt, usually with the anion common to the IL, *e.g.* TFSI, is added to create Li⁺ charge carriers. Unfortunately, ILs tend to be highly viscous, thus limiting conductivity.

One benefit of being able to design ILs, is the possibility to functionalize ILs to act also as redox shuttles,^{131,132} *i.e.* making the solvent its own additive.

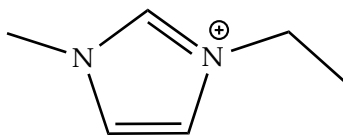


Figure 6: The EMIm cation, 1-ethyl-3-methylimidazolium.

2.3 Sodium-ion batteries

Compared with lithium, sodium is a nigh limitless resource,¹³³ and therefore cheap. Thus, there are economic and environmental incentives to study sodium based batteries. This includes large-scale stationary batteries,¹³ where price and reliability are far more important criteria than energy density.

Sodium battery research has for a long time been largely focused on high temperature batteries ($>160\text{ C}^\circ$), such as beta-alumina sodium batteries, which need an elevated temperature to have sufficient conduction of Na^+ ¹³⁴ and ZEBRA batteries¹³⁵ used in EVs, with an optimum operating temperature range of $270\text{-}350^\circ\text{C}$.

The similarity of the sodium and lithium intercalation chemistry¹³⁶ (known for many decades) opens for the possibility of constructing a sodium-ion battery (SIB), the sodium counterpart of a LIB. However, *a priori* a metallic sodium anode is considered to be quite unsafe due its low melting point (98°C) and the very energetic reaction with water. Furthermore, unlike LIBs a graphite anode can not be used, due to the larger size of Na^+ which prevents reversible intercalation.⁶ Other carbon materials have been explored and the first practical hard carbon (the model for intercalation is seen in Figure 7) was reported by Stevens and Dahn.¹³⁷ While only a proof-of-concept, it showed the potential for SIBs.

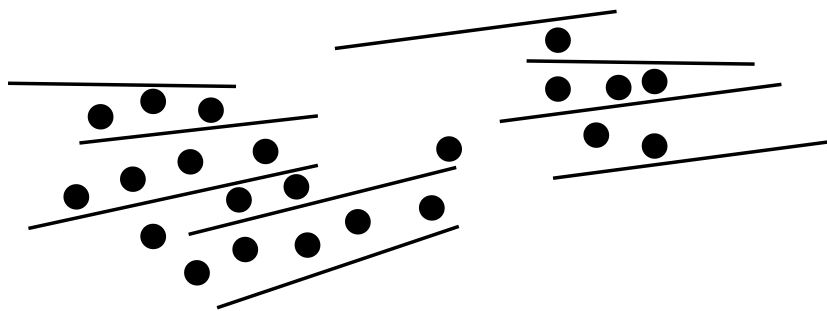


Figure 7: Na^+ intercalation in hard carbon.

The hard carbon anode, unfortunately, suffered from extensive fading during cycling. This can be alleviated with further anode development.¹³⁸ However, Chevrier and Ceder found that using the current anodes systems for Li will give subpar results, thus requiring novel thinking.¹³⁹ A recent paper by Senguttuvan, *et al.*¹⁴⁰ reported their synthesis of a $\text{Na}_2\text{Ti}_3\text{O}_7$ anode (an anode with a low insertion voltage $0.3\text{ V vs. Na}^+/\text{Na}^0$) – alleviating the carbon fading problem by removing the carbon out of the picture.

Barker *et al.*¹⁴¹ found that NaVPO_4F is a promising cathode (they also made a Li analogue⁵²). The study of the cathode materials for SIB can leverage the decades of research on cathodes for LIB, and comparisons can be used to understand their differences.^{142–144}

As the SIBs are still a nascent research topic, the same is true for their electrolytes.^{145,146} Though it is clear that this field is undergoing a quick expansion.^{147,148} Especially as optimisation of the electrolyte can improve the cyclability of the electrodes.^{138,145} This search for optimised electrolytes also includes ILs.^{146,149}

Carbonate solvents, such as EC and PC, have been shown to be promising candidates for SIB electrolytes,^{147,148} with conductivities ranging from 6 mS/cm to 11 mS/cm for 1 M NaClO_4 in a range of carbonate solvent mixtures.¹⁴⁸ Ponrouch *et al.*¹⁴⁸ recommend 1 M of a Na salt (tested both NaClO_4 and NaPF_6) in $\text{EC}_{0.45}:\text{PC}_{0.45}:\text{DMC}_{0.1}$. However, another group has noted cyclability issues for PC on the cathode (in contrast to Ref. 147), this lead to their recommendation of a EC/DEC mixture with NaPF_6 as the salt.¹⁴⁵

2.4 Impact of *ab initio* calculations

The usage of *ab initio* techniques opens up many possibilities related to battery research. They can help understand why certain batteries work the way they do, such as the popular lead-acid battery¹⁵⁰ and the now rare mercury battery.¹⁵¹ Other possibilities range from supporting the interpretation of experimental results to full *ab initio* predictions of novel materials, including phase diagrams,¹⁵² thus enabling high-throughput screening of *e.g.* cathode materials.¹⁵³

Additionally, as synthesis and characterisation of novel materials can be time consuming and very expensive, the possibility to predict properties of novel anions for usage in lithium batteries is valuable. Calculations can give an *a priori* viability of particular anions and thereby guide the synthesis efforts.^{154,155} The pseudo-delocalized anions are a good example of this, as after finding that they are viable LIB electrolyte candidates, efforts to synthesise and characterise them have started. *Ab initio* methods can also guide entry into new fields of research, *e.g.* salts for SIB electrolytes.

The *ab initio* techniques can primarily also be used to augment spectroscopic studies of local and accurate nature, *e.g.* IR, Raman and NMR. For example in Raman spectroscopy, *ab initio* techniques, can simplify peak assignment,¹⁵⁶ or enable a more detailed understanding of conformational equilibria.¹⁵⁷ In a few cases, they can be used by researchers to identify

incorrect interpretations of spectra and correct them.^{116,118} However, this assumes that the theory has only one possible result, which is not the case for the EC/DMC system as seen in Paper IV.

Another application of *ab initio* techniques has been the study of the low level electrochemical processes at the electrode-electrolyte interface. This includes studies of the reductive chemical reactions at the interface,^{34,35} the structure of the interface itself¹⁵⁸ and calculations made to study the role of additives in these processes.¹⁵⁹

However, these techniques need to be used with care and knowledge, as evidenced by a comment by Scheers and Johansson¹⁶⁰ on an article by Li *et al.*¹⁶¹ where incorrect interpretations are due to inaccurate *ab initio* calculations.

Computations involving ILs are far more demanding than for an isolate anion or ion-pairs with Li^+ or Na^+ . This is due to the large number of configurations needed to be explored and the large size of the cations. There are, however, some underlying concerns with the applicability of DFT, due to the long range interactions and the necessity of dispersion correction.¹⁶²⁻¹⁶⁴ Nevertheless, calculations to predict both IR and Raman spectra¹⁶⁵ and the ESWs of ILs have been made, including to reproduce the observed reduction potential of TFSI^{61,166}

Chapter 3

Techniques

This chapter will give a high-level overview of the field of quantum chemistry (QC), while a more detailed account of the techniques used, the following books are recommended: the entry-level introduction book by Atkins and Friedman,¹⁶⁷ the advanced undergraduate/graduate book of Szabo and Ostlund,¹⁶⁸ and for the more advanced learner, the detailed monograph of Helgaker *et al.*, is recommended.¹⁶⁹ Additionally, David B. Cook's book,¹⁷⁰ takes a pedagogical approach to the design and practicalities of quantum chemistry programs.

3.1 The Schrödinger equation

There are numerous approximations used to solve the Schrödinger equation, $E|\Psi\rangle = \hat{H}|\Psi\rangle$. How the Hamiltonian operator, \hat{H} , is constructed has implications for the approximations needed. The common initial approximation is to assume that the nuclear motion and electron motion are separable, the Born-Oppenheimer approximation, *i.e.* nuclear translations are very slow compared to electronic translations. This approximation can, however, be violated during some reactions.^{171,172}

The key difference between Hartree-Fock (HF) and Density Functional Theory (DFT) is how the Hamiltonian is constructed. This difference results in the Roothan-Hall and Kohn-Sham equations (for HF and DFT respectively). Both sets of equations are solved self-consistently; the process of iterative solution that is repeatedly run through the equations until a convergence criteria is reached.¹⁷³

The self consistent field (SCF) loop is an iterative procedure (Figure 8), where a guess for the wave-function is used for calculations according to the equations for HF or DFT (then electron density, ρ). This gives another guess

which again is put through the equations, until they are converged/self consistent. Certain systems can be problematic to converge, due to either a large diffuse basis set or just due to large variations in each iteration step.

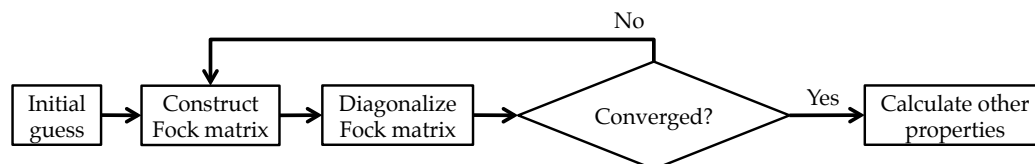


Figure 8: A simplified illustration of the SCF loop.

3.2 Basis sets

For atoms and molecular systems a basis set is used to simplify the Schrödinger equation, by assuming that a linear one-electron basis set is sufficient for the solution, instead of requiring an infinite basis set or a grid based algorithm. The most natural choice for a basis set would be a basis set based on Slater type orbitals (STO)

$$\eta_{STO}(\alpha) \propto \exp(-ar)$$

They are a natural choice, as they are the solution to the only known solution to the Schrödinger equation, the hydrogen atom. Thus STOs have the expected behaviour of an all electron wave-function, *i.e.* are anti-symmetric (as required by the Pauli exclusion principle), decay to 0 at $\pm\infty$ and have a cusp at the origin/nucleus.

However, as any calculations with STOs are non-trivial as all integrals have to be tackled numerically, other options have emerged, primarily the common Gaussian-Type Orbital (GTO) basis sets. GTO basis sets are constructed from functions, that have the same properties as gaussian distributions, as visualised in Figure 9. As the overlap of two gaussian functions is a gaussian function, a number of the formulas can be solved analytically, as suggested by Boys.¹⁷⁴

Thus GTO basis sets are constructed from primitive gaussians:

$$\eta(\alpha) = N \cdot x^l y^m z^n \cdot \exp(-ar^2)$$

where N is a normalisation factor, $x^l y^m z^n$ is a cartesian factor and α is the gaussian exponent (sometimes written as ζ).

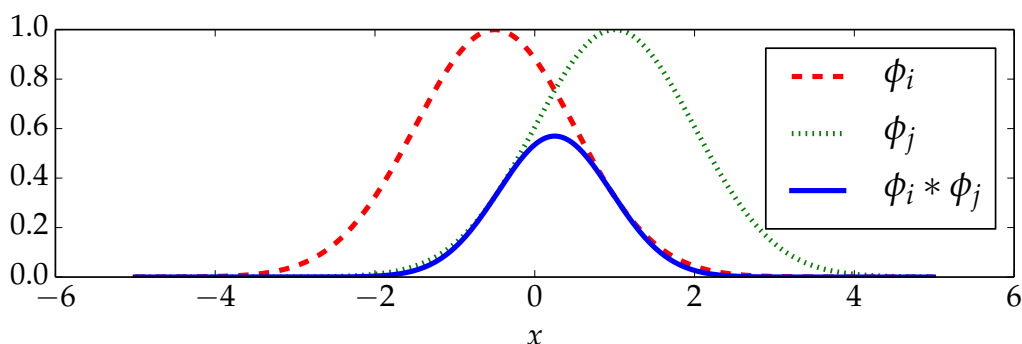


Figure 9: The overlap, $\phi_i * \phi_j$, of two different gaussian functions, ϕ_i and ϕ_j , is a gaussian.

These primitive gaussians are usually put together in a contracted gaussian basis set, where each contracted gaussian basis function is a linear combination of primitives:

$$\phi_i = \sum_{k=1}^K \eta_k d_{ki}$$

where d_{ki} is a contraction coefficient. These contraction coefficients are held as constants through the entire calculation. The contracted gaussian set is then combined from a number of contracted gaussians:

$$\psi = \sum_i^N c_i \phi_i$$

These c_i are parameters that are optimised in quantum chemistry calculations.

STO- n G was the first systematic gaussian basis sets which was constructed to replace Slater-type orbitals.¹⁷⁵ For example, the STO-3G can be considered a minimal basis set, that can be used for test calculations.

A subsequent development was to split apart the basis set, in a manner such that the valence and core electrons are treated separately. This results in a split valence basis set. The common $X - YZG$ Pople basis sets are of this variety. They have a single basis function, which is constructed from X primitive gaussian functions in the core; each valence orbital is split into two, one part made of Y gaussian functions and another made of Z gaussian functions. The first reported basis of this type was the 4-31G basis set,¹⁷⁶ a later addition was the 6-31G¹⁷⁷ which has proven to be fairly popular. To

improve these basis set, especially for anionic species (where the HOMO electrons may be localized over a large space), they are augmented with a diffuse gaussian function.¹⁷⁸ These basis sets are usually denoted with a plus, *i.e.* 6-31+G¹⁷⁹ (if included also on hydrogen, then ++).

A further improvement on the basis sets is to add functions that allow for a polarisation of the orbital by distortion. For the Pople basis sets, a basis set with polarisation function has an asterisk in its name, *e.g.* 6-31G* (if there are two asterisks, then hydrogen also has a polarisation function).¹⁸⁰

Another property that is important to note about basis sets, is the multiplicity of the zeta*, *i.e.* how many gaussian functions are used to construct each electron's valence shell. Thus a double zeta basis set, such as 6-31G, has 2 gaussian functions, one constructed from three primitive gaussians and another made from a single primitive gaussian. 6-311G would accordingly be a triple zeta basis set.

3.2.1 CBS limit

As the basis sets used in quantum chemistry are an approximation of a complete basis set (CBS), there are bound to be errors – especially as the design criteria for a basis set can be conflicting.¹⁸¹ However, by using systematic basis sets, *i.e.* a truncated part of an infinite series, and the associated systematic error reduction in energies, approximate energy values at the CBS limit can be obtained by extrapolation.

Figure 10 shows the effect of increasing the basis set size on the electron density for hydrogen fluoride. The larger basis sets allow the electrons to be localized more on the fluorine atom. The difference between a TZ basis set and 5Z basis set is not large, a TZ basis set can thus be sufficient.

Key basis sets used for CBS calculations are the Dunning correlation consistent basis sets¹⁸² and the polarization consistent basis set of Jensen.¹⁸³ They are constructed in a systematic manner that enables an approximation of the CBS limit. However, these two sets have different aims, the former is aimed for applications involving CI/CC methods (see Section 3.3.2), while the latter is aimed at HF and DFT methods.

3.3 Wave-function methods

Quantum chemical methods can be split into two main *ab initio* branches, the wave-function methods and the density methods. As the names

*ζ, the greek letter zeta, is often used in mathematics as the exponent constant of gaussian functions.

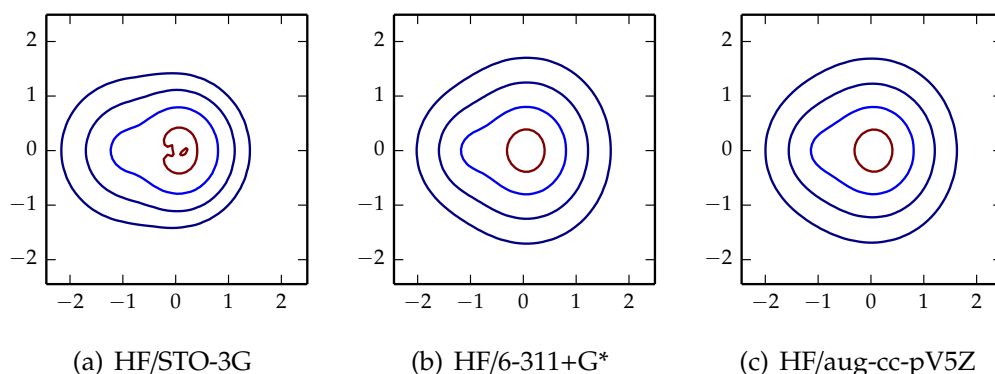


Figure 10: A contour plot of the electron density of hydrogen fluoride, calculated with HF/STO-3G, HF/6-311+G* and HF/aug-cc-pV5Z. The contour lines are at fixed values ($10^n \text{ e}/\text{\AA}^3$, $n = -3, \dots, 0$). The fluorine atom is at the origin and the hydrogen atom is 0.95 \AA away.

suggest, the wave-function methods are built around wave-functions, Ψ , and density methods around the electron density, ρ . The wave-function methods include HF, Configuration Interaction (CI) and Coupled Cluster (CC). Density methods are all variations of DFT which lays the groundwork for the various functionals.

The wave-function methods are built around wave-functions that are Slater determinants:

$$\Psi = \Psi(1, 2, \dots, N) = \frac{1}{\sqrt{N!}} \begin{vmatrix} \phi_1(1) & \phi_2(1) & \cdots & \phi_K(1) \\ \phi_1(2) & \phi_2(2) & \cdots & \phi_K(2) \\ \vdots & \vdots & & \vdots \\ \phi_1(N) & \phi_2(N) & \cdots & \phi_K(N) \end{vmatrix}$$

where $\phi_k(i)$ is a spin-orbital k of electron i . The Slater determinants are antisymmetric and fulfil the Pauli exclusionary principle (if $i = j$, then no wave-function).

3.3.1 Hartree-Fock, 2nd order Møller-Plesset and Configuration Interaction

The HF equations replace the Schrödinger equation with an eigenvalue problem:

$$f|\chi_a\rangle = \epsilon|\chi_a\rangle$$

where χ_a is a spin-orbital, ϵ are the orbital eigenvalues and f is the Fock operator:

$$f(i) = h(i) + v_{HF}(i)$$

where $h(i)$ is the kinetic energy of electron i of N with M nuclei:

$$h(i) = -\frac{1}{2}\nabla_i^2 - \sum_A^M \frac{Z_A}{r_{iA}}$$

and v_{HF} is the HF potential:

$$v_{HF}(i) = \sum_{b \neq a} J_b(i) - \sum_{b \neq a} K_b(i)$$

The terms, that the HF potential is made of, are the Coulomb operator, $J_b(i)$, and the exchange operator, $K_b(i)$. These equations are solved self-consistently (Figure 8). In general, the Roothaan-Hall equations^{184,185} (independent discovery) are used, which transform the HF equations to an eigenvalue problem in a basis set.

HF performs in a way remarkably well, as it recovers nearly all of the electronic energy. The key deficiency of HF is the lack of electron-correlation as HF ignores the complex interaction between two electrons.

One post-HF method with electron-correlation is CI. At its core, it is a linear combination of all Slater determinants of an N -electron system, which is then solved variationally:

$$\Psi = C_0\Phi_0 + \sum_{a,p} C'_a\Phi_a^p + \dots$$

where Φ_0 is the HF solution and Φ_a is the a -th one electron excitation. A full Configuration Interaction (FCI), does this for all N electrons and all possible excitations of the system. It is, however, an extremely expensive method, not practical for anything but tiny systems.

Another method, which is used to recover the correlation energy, is cheaper in computation than CI and does it perturbatively. This is done with Møller Plesset Perturbation Theory (MPPT). Møller and Plesset¹⁸⁶ pioneered this approach to the HF equations in 1934. The degree of the perturbation determines the theory level, *i.e.* MPn is a Møller-Plesset theory calculation of degree n . The energy of the system is then $E = E_{HF} + E_{MP2}$. With the energy of the perturbation term (given in chemists' notation¹⁶⁷):

$$E_{MP2} = \frac{1}{4} \sum_{a,b}^{occ} \sum_{p,q}^{virt} \frac{(ab||pq)(pq||ab)}{\epsilon_a + \epsilon_b - \epsilon_p - \epsilon_q}$$

MP2 is clearly the most popular of the perturbation methods. While one could intuitively expect that a higher level of perturbation would give increasingly better results, in exchange for more computing, this is not necessarily the case. MP3, for example, can perform worse and better than MP2, same goes for MP4. Thus one can not say MP_{n+1} is always better than MP_n . This oscillatory behaviour of diminishing returns can be seen in an article by Hirata and Bartlett.¹⁸⁷ For the current state of the field of MP_n calculations, the recent review by Cremer¹⁸⁸ is recommended.

3.3.2 Coupled Cluster

Another corrective method for HF is the CC method. This method starts from a HF solution, Ψ_0 , and uses a cluster operator \hat{T} to correct that solution:

$$\Psi = e^{\hat{T}}\Psi_0, \quad \hat{T} = \sum_{i=1}^N T_i$$

Each term, T_i , of the cluster operator functions as an electron excitation operator of order i . Thus T_3 would be a three electron excitation operator. A schematic depiction of the effect of these operators can be seen in Figure 11.

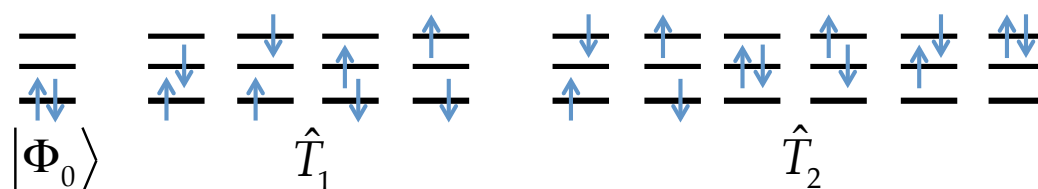


Figure 11: The cluster operator $\hat{T} = \hat{T}_1 + \hat{T}_2$ acting on a two electron ground state $|\Phi_0\rangle$ with two virtual orbitals.

The cluster operator is finite, only N electrons to excite, nevertheless if all electron excitations were taken into account the cost would be prohibitive[†]. Thus the cluster operator is truncated, a common version in usage is $\hat{T} = T_1 + T_2$, which is known as coupled cluster singles doubles (CCSD). A fair approximation, as most of the correlation energy comes from two electron interactions.

CC theory forms a very powerful set of methods, due to its convergent behaviour. CC is conceptually similar to CI, but the exponential factor of

[†]Note that $CC(N)$ of a N -electron system is the same as a FCI of the same system.

the cluster operator has considerable impact. CI is not size-consistent[‡], while CC is.

The reference method of choice,¹⁸⁹ however, is the CCSD(T) method. This method starts with a CCSD calculation and adds in the triple electron excitations perturbatively. Where CCSD is not precise enough and while CCSDT is precise enough, but too expensive, the CCSD(T) method bridges this gap.¹⁶⁹ This method is often coupled with a series of basis sets to calculate a CCSD(T)/CBS value.

For more, see the introduction to CC by Bartlett,¹⁸⁹ the book chapter by Crawford and Schaefer¹⁹⁰ or the review by Bartlett and Musiał.¹⁹¹

3.4 Density Functional Theory

The Hohenberg-Kohn theorem¹⁹² proves that there exists a functional for a ground state that is entirely determined by the electron density, ρ , of a N electron system, *i.e.* the properties of the ground state can be derived from just ρ :

$$\rho(r) = \sum_{i=1}^N |\phi_i(r)|^2$$

Their proof was unfortunately a proof of existence, not a constructive proof. The subsequent development of the eponymous Kohn-Sham equations¹⁹³ made modern density functional theory (DFT) possible:

$$\left\{ -\frac{1}{2}\nabla^2 + [\phi(r) + V_{xc}(\rho(r))] \right\} \psi_k(r) = \epsilon_k \psi_k(r)$$

Note that this equation is very similar to the Hartree-Fock equation (and can be solved in the same self-consistent manner), but with a very important extra term; the exchange-correlation potential, $V_{xc}(\rho(r))$. This term is what is approximated with the various functionals of DFT.

3.4.1 Functionals

There is a large number of functionals available for DFT calculations, each with its own pros and cons. They can be systematically categorised and fortunately, their performance tends to follow the category. However, there is still no systematic way to improve the functionals.

[‡]Size-consistent: For two fully separated system A and B, $E_{AB} = E_A + E_B$.

One classification scheme is the, biblically inspired analogy of, Jacob's Ladder of Perdew and Schmidt.¹⁹⁴ There, the functionals are ordered according to the increasing complexity of the approximation. This classification has been shown to correlate with functional performance,¹⁹⁵ which also is investigated in Paper V.

A local density functional, where V_{xc} only depends on the value of $\rho(r)$ in each point, is at the bottom rung of the ladder, *i.e.* LSDA.

At the second rung the gradient of the electron density, $V_{xc}(\nabla\rho(r), \rho(r))$, is added – these functionals are called General Gradient Approximation functionals (GGA), these include BLYP^{196,197} and PBE.^{198,199}

At the third rung are the meta General Gradient Approximation functionals (meta-GGAs) which add the kinetic energy density, $\tau_{\sigma}(r)$ of the electrons into the mix. Meta-GGAs include VSXC,²⁰⁰ M06-L²⁰¹ and TPSS.²⁰²

The pure functionals, such as PBE and TPSS, are constructed by utilising some of the known properties of the exact DFT functional, which have been explored by *e.g.* Levy²⁰³ and Levy and Perdew.²⁰⁴ This information has then been incorporated into functional development, thereby eschewing empiricism. However, at the fourth rung of the ladder, no functionals without empiricism have been developed, an ongoing problem in research.²⁰⁵

The fourth rung has the hyper-GGAs, where exact exchange is used, *i.e.* the HF exchange. These include B3LYP,^{197,206,207} the most popular functional in chemistry, M06,²⁰¹ BMK²⁰⁸ and TPSSh.^{202,209} These are generally referred to as hybrid functionals.

The fifth rung adds in unoccupied Kohn-Sham orbitals, these include B2-PLYP,²¹⁰ XYG3²¹¹ and DSD-PBEP86.²¹² Double-hybrid functionals, as proposed by Grimme,²¹⁰ include a perturbation step (of the second order) to improve calculations. Thus the exchange-correlation energy of a GGA based double hybrid is:

$$E_{XC} = (1 - a_x)E_x^{GGA} + A_x E_x^{HF} + bE_c^{GGA} + cE_c^{PT2}$$

Note that if $c = 0$ then it would be a hybrid, not a double hybrid. However, these functionals are very expensive due to the scaling of their perturbative step (E_c^{PT2}). This rung also includes the random phase approximation (RPA) functional.²¹³

The performance of DFT for the calculation of most properties can be very good, as evidenced by the recent benchmarks done by Goerik and Grimme.^{214,215} However, a key problem that affects the performance is the self-interaction error.^{216,217} This is due to that a single electron is included in the electron density and thus when it interacts with the density, it is also interacting with itself. Some corrections have been developed to

compensate,²¹⁸ however, it was only discovered recently that the corrections require complex orbitals.²¹⁹ Another issue is that the grid (used for numerical calculations), can have an impact.²²⁰

Another type of functionals have an empirical term that corrects the long-range behaviour of the functional. These include the dispersion corrected functionals of Grimme *et al.*, such as B3LYP-D.^{221,222}

Functional performance and selection

With so many functionals, some rational criteria for the selection of a functional must be used. As the Jacob's ladder gives a rough mapping of performance, going as high as possible would be preferable. At the fifth rung, the double hybrids have excellent performance, however, using these functionals can be impractical due to the computational expense[§].

Thus if one looks in more detail at a couple of functionals at lower rungs:

VSXC has been used for the calculation of intrinsic anions oxidation potentials⁶⁴ due to its good performance with IP/EA calculations.²²³

Unfortunately, it is plagued by convergence issues, both during geometry optimisation and SCF convergence - to the extent that a benchmarking study simply removed it from their analysis.²¹⁴

B3LYP is not the best, but still good enough for many applications. The first hybrid (explored the role of exact exchange), which is now 20 years old, and still has not been supplanted. However, considering the improvements made in the last two decades, it should, untested, not be the sole functional used.

M06-2X is a possible replacement for B3LYP, and has been shown to perform fairly well during benchmarks. However, as it is a heavily parametrized functional, the corner cases of the functional must be explored further before it can be accepted fully. When combined with a dispersion correction, it has been shown to perform best of all hybrids.²¹⁴

M06 is functional similar to M06-2X with a slightly different design goal; optimised for compounds that include transition metals, unlike M06-2X which has been optimised for main-group chemistry.

[§]For the BPFPPB anion, replacing the B3LYP functional with the B2PLYP functional, the CPU time increased by a factor of 17.

M06L is another variation where no exact exchange is used and therefore the calculations are simpler, *i.e.* require less CPU power. Despite this it can in some cases surpass B3LYP in performance.²²⁴

3.4.2 Hardness and softness

Parr *et al.* identified that the connection between DFT and electronegativity, χ in 1978:²²⁵

$$\chi = -\mu = -\left(\frac{\partial E}{\partial N}\right)$$

where μ is the chemical potential and N is the number of electrons. This was then extended in such a way to connect DFT to the theory of hard and soft acids and bases, to give an absolute hardness^{226,227} and Fukui functions.^{228,229} The hardness, η is defined as:

$$\eta = \frac{1}{2} \frac{\partial \mu}{\partial N} = \frac{1}{2} \left(\frac{\partial^2 E}{\partial N^2} \right)_{v(r)}$$

This field has been called conceptual density functional theory,^{230,231} and is here used in Paper V.

3.5 CBS methods

Many methods have been designed to calculate the energy at the CBS limit (discussed in section 3.2.1). These methods require a series of calculations with successively larger basis sets. Since the energy is extrapolated to infinity, there are a number of choices for extrapolation formula.

An early single exponential form of the formula was reported by Feller:^{232,233}

$$E = a + b \exp(-cn)$$

where n is the cardinal number of the basis set, *i.e.* two for cc-pVDZ, etc. Halkier *et al.*²³⁴ note that this form works well for HF energies. Peterson *et al.*²³⁵ proposed the following double exponential form:

$$E(n) = E_{CBS} + A \exp[-(n-1)] + B \exp[-(n-1)^2]$$

Helgaker *et al.*²³⁶ proposed using a different form just for the correlation energy:

$$E_{corr} = a + bn^{-3}$$

For a thorough analysis of the performance of the power form and the single exponential form formulas, see Halkier *et al.*²³⁴ Both the single exponential and the power form have been shown to work fairly well. While depending on the accuracy needed and computational resources available, other extrapolation methods might be required.²³⁷ Below two such methods are outlined.

3.5.1 Composite methods

Composite methods aim to get excellent results by combining a number of calculations using various methods, *i.e.* high-level methods with small basis-sets and vice versa. They might then use a corrective empirical term for the system.

One example is the G_n ($n = 1 - 4$) methods,²³⁸ a reasonably costly set of methods[¶]. The $G3$ ²⁴⁰ method is a popular version, despite its inclusion of a fairly expensive quadratic CI step. The $G4$ ²⁴¹ is a newer method designed to supplant the $G3$. The $G4MP2$ ²⁴² supplements $G4$ as it is a cheaper variant of $G4$ ($G4MP2$ has no MP4 step). $G4MP2$ notably outperforms $G3$, despite being cheaper computationally. These methods are applied in Paper III.

3.5.2 Approximate CBS

While CCSD(T)/CBS is seen as a gold-standard, it can be very expensive to calculate, especially at the quadruple or quintuple zeta level. Thus, an approximation of the CCSD(T)/CBS is used in this thesis. It uses the following correction term

$$\Delta\text{CCSD(T)} = E_{\text{CCSD(T)}}^{\text{small}} - E_{\text{MP2}}^{\text{small}}$$

Thus the estimated CCSD(T)/CBS value is:

$$E_{\text{CCSD(T)}}^{\text{CBS}} = E_{\text{MP2}}^{\text{CBS}} + \Delta\text{CCSD(T)}$$

where $E_{\text{MP2}}^{\text{CBS}}$ has been extrapolated to the CBS limit. As MP2 calculations scale better than CCSD(T), an estimate of the CCSD(T)/CBS energy is feasible for fairly large systems.²⁴³

[¶]Note that G_n (in combination with a year) can also refer to a test set of molecules, such as $G3/99$.²³⁹

3.6 Atoms in molecules

To find the atomic charge in a molecule several approaches have been proposed. One of these is Bader's Atoms in Molecules (AIM).²⁴⁴ It works by dividing space into volumes that are separated by zero-flux boundaries. These volumes then contain the electrons localized to atoms, and thus the atomic charge is found by integration of the electron density over the volume. By further analysis, bonds can also be located.²⁴⁵

Recent algorithm development has reduced the computational effort of AIM analysis, thus enabling more usage of this approach.^{246–248}

3.7 Derivatives

In this chapter, many different QC methods have been discussed. One very important part of their calculations is, however, yet to be discussed – the derivatives of the energy. These can be calculated numerically with the standard finite difference schemes or they can be calculated with analytical formulas.

Pulay played a key role in the development of the analytical derivatives²⁴⁹ for QC methods. Though he was not the first to describe them, he was first to show that gradient calculations from HF solutions were comparatively simple.²⁵⁰

The key advantage of using analytical derivatives is the small computational effort as all the first derivatives are calculated at once, instead of having to do a full SCF calculation for each degree of freedom. Another advantage is that there is less numerical instability due to the finite difference scheme employed.²⁵¹

3.7.1 Optimisation

$\partial E/\partial \mathbf{R}$, the first derivative of the energy with respect to nuclear coordinates, \mathbf{R} , is the derivative that almost all QC program users will encounter. This is due to its use in geometry optimisation,²⁵² where the gradient is used to get information about the potential energy surface so that a energy minimum can be found. However, many minima can exist on a potential energy surface (as seen in Figure 12), thus finding the global energy minimum is not guaranteed.

In general, methods from numerical analysis are used for this optimisation, such as the quasi-Newton methods. These methods approximate the Hessian matrix via some update scheme, such as Broyden-Fletcher-

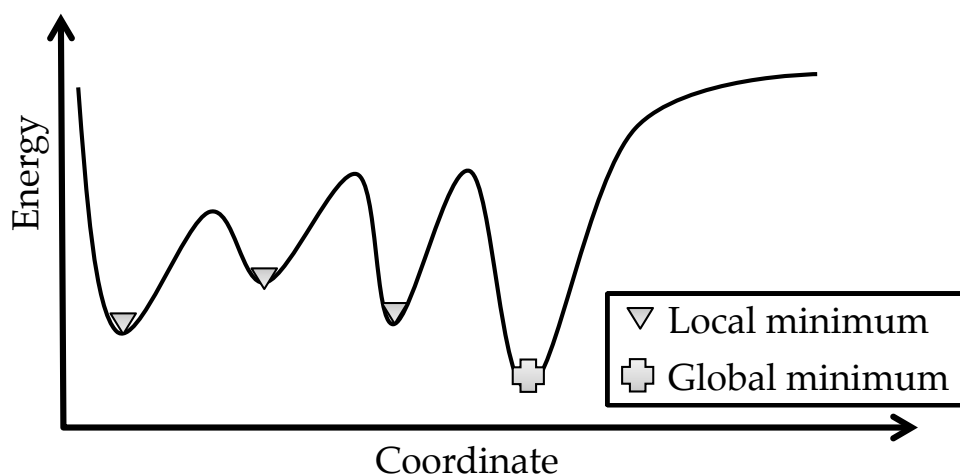


Figure 12: Here is an imaginary system which has a number of local minima and one global minimum.

Goldfarb-Shanno (BFGS). This allows for a fast convergence without having to recalculate the Hessian at each step as for the Newton method.

3.7.2 Spectra

Once a structure has been optimised, it is usually verified to be a minimum by calculating the vibrational frequencies of the molecule^{||}. This is done by calculating the Hessian, *i.e.* $\partial^2 E / \partial \mathbf{R}^2$, for the molecule (at this geometry). Then the frequencies are calculated via the harmonic approximation. If any of the frequencies are imaginary, then this is not a minimum (ignoring numerical issues). If there is only one such frequency, then it is a transition state.

These frequencies can then be used for thermochemistry calculations, *e.g.* to calculate the enthalpy of the molecule²⁵³ or together with intensities be useful for different kinds of spectroscopy. To get the IR intensities, another derivative must be calculated: $\partial^2 E / \partial \mathbf{R}_i \partial \mathbf{F}$, where \mathbf{F} is the external electrical field. This derivative is proportional to the change in the dipole moment during vibration – revealed by IR spectroscopy. If Raman intensities are also needed, then $\partial^3 E / \partial \mathbf{R} \partial \mathbf{F}^2$ is used, which is proportional to the polarizability change of the molecule. Indeed, also other spectra can be calculated, such as NMR, which uses the derivative of the energy with respect to the magnetic moment of the molecule and the magnetic field.²⁵⁴

^{||}This checks whether it is a minimum, not the global minimum.

Chapter 4

Applications and Results

Ab initio methods (see Chapter 3) are here employed to describe the inner workings of the electrolyte at a molecular level, by various approaches. The conductivity is targeted by the ion pair dissociation energy (Section 4.1) and the solvation energy (Section 4.2). The stability of the salt can be split into electrochemical and thermal stability. The oxidation potential of the salt is discussed in Section 4.3, while the thermal stability and the breakdown products are discussed in Section 4.4. For certain systems additional properties are introduced, *e.g.* for the pseudo-delocalized anions a charge localization method (Section 4.5). When nothing else is stated the Gaussian program suite²⁵⁵ was used for all the *ab initio* calculations.

4.1 Ion-pair dissociation energy

High conductivity in an electrolyte requires that charge carrying species can easily be created. This requires the dissociation of a salt into the cation (here either Li^+ or Na^+) and anion, which is dependent on using weakly coordinating anions. In addition, the solvent used must solvate the cation (and anion) to accomplish this "charge separation" (the solvation is discussed in Section 4.2). These processes are shown schematically in Figure 13.

Focusing on the cation-anion dissociation part, a measure can be designed; the ion-pair dissociation energy, ΔE_d . This measure can be used both for lithium and sodium salts:

$$\Delta E_d = E_{\text{Alk}^+} + E_{\text{An}^-} - E_{\text{AlkAn}}$$

where Alk is either Li^+ or Na^+ . This measure is used extensively in Paper I-III. In Paper I and Paper Paper II, ΔE_d is only calculated for lithium cation-

anion ion-pairs, while in Paper III, it is done for both lithium cation-anion and sodium cation-anion ion-pairs.

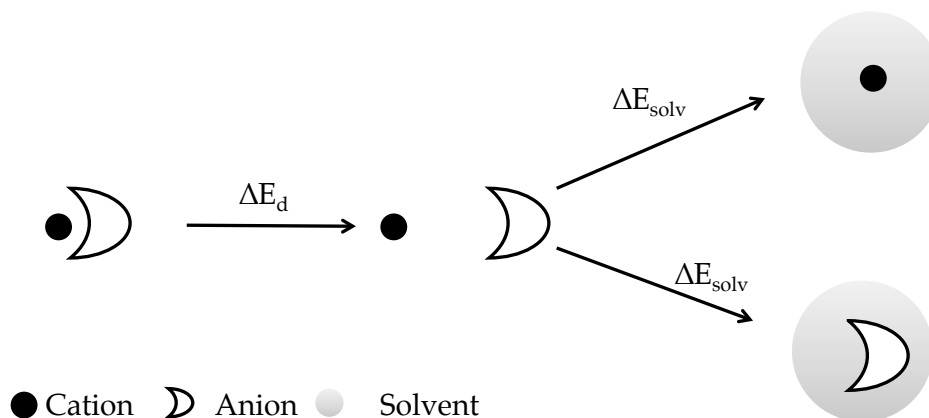


Figure 13: The making of charge carriers. An endothermic initial step of ion-pair dissociation, ΔE_d , is followed by exothermic solvation, ΔE_{solv} , steps for both the separated ions. The ΔE_d and the ΔE_{solv} cation are of similar magnitude.

The lowering of ΔE_d can have a dramatic effect on the conductivity as can be seen by going from LiBBB ($\Delta E_d=579$ kJ/mol) to Li4F-BBB ($\Delta E_d = 497$ kJ/mol).⁸¹ This increased the conductivity by 260% in DMC/EC, while all other structural parameters were kept constant.⁸⁰ Therefore the lowering of ΔE_d has been shown to have an effect on the conductivity, thus studies on electrolyte salts can (at least in part) focus on the ion-pair dissociation energy.

One key difficulty arises in ΔE_d calculations: the problem of finding the ion-pair structure with the lowest energy. Many anions of interest for LIBs or SIBs have a number of possible coordination sites available (as outlined in Figure 14), which must all be explored. Even though optimisation algorithms used in quantum chemistry programs are very advanced, most work only locally, always decreasing the energy of the system, and thus find minima not being the global energy minimum. Thus, here two main approaches are used to find the global minimum, either to use chemical intuition to predict a number of likely starting structures or *via* brute force with the use of a structure randomiser, such as SECIL.^{256,257} The latter approach was employed almost exclusively in papers II and III.

One of the key benefits of the mindless exploration²⁵⁸ of SECIL of the potential energy surface of the ion-pairs is the identification of non-obvious structures. As the program explores until it can not find any new unique

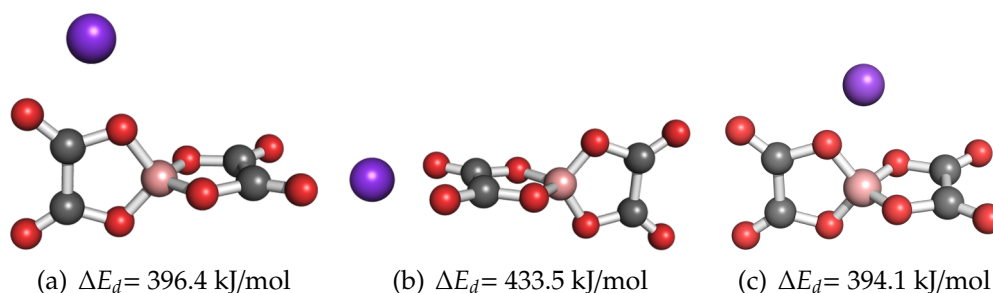


Figure 14: The ion-pairs of NaBOB

structures, it is unlikely that it misses any minima. The discovery of such non-obvious structures is described in both Paper II and Paper III.

In Paper II we found that one of the factors affecting the ΔE_d of the pseudo-delocalized anions is the flexibility of the negative moieties. This increases the ΔE_d as the Li^+ ion is coordinated stronger than expected. In Paper III, a few sodium ion-pair structures were found that would not have been found by just using chemical intuition. These structures were not found during a prior study with lithium ion-pairs,⁸¹ perhaps due to being only feasible with a larger cation.

By calculating the ΔE_d for the pseudo-delocalized anions, some were found to be interesting candidates for synthesis, having lower ΔE_d values than LiPF_6 (567 kJ/mol), *e.g.* 1,3S5MePy (542.0 kJ/mol), SSA (546.9 kJ/mol) and 1,3SIIm (546.6 kJ/mol).

Paper III explored the difference of the ΔE_d for lithium and sodium ion-pairs. In general one can expect a sodium salt to have $\approx 80\%$ of the ΔE_d value of the corresponding lithium salt. This 80% trend can also be seen for the sodium salts of the pseudo-delocalized anions, with previously unreported data to be found in Appendix B.

4.2 Solvation energy

The dissociation of the electrolyte salt is concerted with the solvation of the cation and anion, where the energy of solvation, $\Delta E_{\text{solv cation}} \gg \Delta E_{\text{solv anion}}$.²⁵⁹ Thus, the solvation of the cations, both Li^+ and Na^+ , is the focus here.

Addressing in detail the structure of the solvation shells of the cations requires explicit solvation calculations. A measure of solvation energy is required, and there are at least two obvious definitions of solvation energy. In Paper IV, the first definition of the solvation energy is :

$$\Delta E_{\text{solv}} = E_{\text{Alk}(\text{EC})_x(\text{DMC})_y} - (E_{\text{Alk}} + x * E_{\text{EC}} + y * E_{\text{DMC}})$$

while the second, the binding energy, is:

$$\Delta E_{bind} = E_{Alk(EC)_x(DMC)_y} - (E_{Alk} + E_{(EC)_x(DMC)_y})$$

In these formulas, $E_{Alk(EC)_x(DMC)_y}$ is the energy of the optimised cation-solvent complex, $E_{(EC)_x(DMC)_y}$ is the energy of the complex without the cation, E_{EC} and E_{DMC} are the energies of the EC and DMC molecules, respectively.

The first definition, *i.e.* ΔE_{solv} , is the intuitive definition of solvation energy. However, the latter definition, *i.e.* ΔE_{bind} , has one key advantage over ΔE_{solv} , it reduces the energy variations due to the solvent-solvent interaction – important for cation-solvent studies.

ΔE_{solv} and ΔE_{bind} were used to explore the solvation of Li^+ and Na^+ in an EC/DMC solvent mixture. By using the fast DFT code Terachem,^{260,261} it was possible to explore a large number of candidates for the solvation structure for both cations, and the coordination number (CN=4) was found to be most realistic. Likely solvate structures for Li^+ were identified to be $Li(EC)_2(DMC)_2^+$ ($\Delta E_{bind} = -731.6$ kJ/mol), $Li(EC)_3(DMC)^+$ ($\Delta E_{bind} = -725.2$ kJ/mol) and $Li(EC)_4^+$ ($\Delta E_{bind} = -719.3$ kJ/mol). Na^+ had $Na(DMC)_4^+$ ($\Delta E_{bind} = -621.6$ kJ/mol), $Na(EC)(DMC)_3^+$ ($\Delta E_{bind} = -614.5$ kJ/mol) and $Na(EC)_2(DMC)_2^+$ ($\Delta E_{bind} = -608.4$ kJ/mol). Thus, there is no strong selective solvation for either cation, rather many possible solvation shells.

As the fast DFT code had limited precision, higher level calculations were applied for a more detailed study of the CN=4 system. Additionally, the different coordination sites of DMC (due to its conformational equilibrium) were explored. This resulted in quite different results as the different coordination sites of DMC have very different affinities for cation coordination. Thus it is predicted that $Li(DMC)_4^+$ ($\Delta E_{bind} = -645.2$ kJ/mol, all DMC in trans-trans conformers) is the most likely solvate structure, while the structure favoured in the literature, $Li(EC)_4^+$ is far higher in energy ($\Delta E_{bind} = -626.0$ kJ/mol).

Similar features were seen for Na^+ , where $Na(EC)_1(DMC)_3^+$ ($\Delta E_{bind} = -516.6$ kJ/mol, all DMC in trans-trans) was the solvate lowest in energy. Other structures were $Na(DMC)_4^+$ ($\Delta E_{bind} = -514.8$ kJ/mol, 2 DMC in trans-trans, 2 in cis-trans) and $Na(EC)_1(DMC)_3^+$ ($\Delta E_{bind} = -513.6$ kJ/mol, 2 DMC in trans-trans, 1 in cis-trans). However, it was also revealed that the CN for Na^+ is more sensitive to the level of theory used, and finally a large solvate with CN=6 is expected from the detailed calculations.

Experimental verification

Paper IV has predictions which should be directly observable in spectroscopic experiments as the various DMC containing cation-solvent complexes

have noticeable differences in their vibrational frequencies. It must be noted that the different conformers of DMC, each have their spectral signature, both as a pure solvent and as a cation-solvent complex. This gives a strong guidance for experimental verification, *i.e.* Paper VII.

The Raman spectra of the Li^+ and Na^+ cations in EC/DMC were calculated for a simple model of a cation with one solvent molecule only. These spectra were then used to guide the interpretation of the measured spectra. This allowed for the identification of the coordination peaks of DMC for both DMC cis-cis and cis-trans conformers. However, there was no sign of the DMC trans-trans peak, which differs from the B3LYP results of Paper IV which predicts a dominance of trans-trans conformers.

The measured solvation contribution of DMC for the solvation of Li^+ in the 1:1 EC/DMC blend is 1.22, which is split into a contribution from the cis-cis, 1.00 and cis-trans, 0.22. While for the Na^+ case DMC cis-cis contributes 1.15, and cis-trans 0.08. These numbers are in line with the predictions made on the smaller system (calculated in Paper VII) as the change in the conformational equilibrium of DMC is smaller for Na^+ than for Li^+ . If one allows for some error, *e.g.* 1%, for the ΔE_{bind} value of Paper IV, then the predictions would be somewhat closer with the experimental values. This comes from the large number of very close values, however, that does not explain the B3LYP prediction that $\text{Li}(\text{DMC})_4^{\text{TTTT}}$ should dominate. Most likely, this is an effect from the solvent-solvent interactions, which could perturb these values even further.

4.3 Oxidation potential

The initial work by Kita *et al.*^{70,262} and Barthel *et al.*⁷⁹ are early examples of using *ab initio* calculations to study the oxidative stability of anions, by using the HOMO energy, E_{HOMO} , where it was found that E_{HOMO} correlates with the oxidation potential. This is a consequence of the Koopmans' theorem,²⁶³ which states that the ionisation potential is the E_{HOMO} . Ue *et al.*²⁶⁴ pioneered the systematic *ab initio* study of the oxidative stability of anions for lithium batteries. As the Koopmans' theorem does not hold for DFT calculations (though this is a point of debate in the literature²⁶⁵⁻²⁶⁷), Ue *et al.* instead used the vertical ionisation potential, ΔE_v . Even more systematic studies were done by Xue and Cheng²⁶⁸ and Johansson.⁶⁴

ΔE_v , is calculated as:

$$\Delta E_v = E_{\text{radical}} - E_{\text{ground state}}$$

where E_{radical} is the energy of the radical that has the same geometry as the

anion, *i.e.* the Frank-Condon approximation (see Figure 15). This differs from the ionisation potential, IP, which involves a geometry optimisation of an excited state (which can be expensive to calculate).

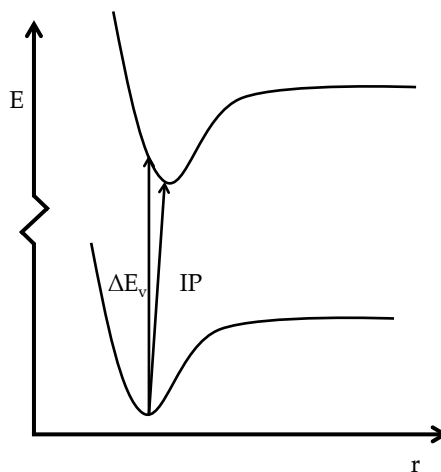


Figure 15: The difference between the vertical ionisation potential, ΔE_v , using the Frank-Condon approximation and the true ionisation potential, IP, is the geometry relaxation of the excited state.

ΔE_v is useful to gauge the intrinsic electrochemical stability of novel electrolyte anions, due to the practical issues that confound the measurements of oxidation potentials, E_{ox} , of anions. The salts of the anions must be dissolved in some solvent, which also may react electrochemically and not be distinguished from the oxidation reactions of the anions.⁷⁶ The electrodes used can also have an effect on the measured oxidation potentials.²⁶⁹ Furthermore, the cutoff current density is not scientifically based.²⁷⁰

In the literature E_{ox} values are given relative to a potential, with the reference in the LIB literature being Li^+/Li^0 . ΔE_v values are, however, absolute, *i.e.* must be shifted to be comparable with Li^+/Li^0 . The shift is -1.46 eV;²⁷¹ approximately the difference between the absolute potential standard hydrogen electrode (-4.44 V²⁷²) and the standard reduction potential of Li (-3.04 V).

The ΔE_v approach of predicting the anion oxidation potential was used in Paper II for pseudo-delocalized anions, revealed to have in general $\Delta E_v \approx 3.5$ V vs. Li^+/Li^0 . However, there were a couple of outliers, both with a very low value such as 1,3OIm with $\Delta E_v = 0.74$ V vs. Li^+/Li^0 and with a high value such as SSP with $\Delta E_v = 4.45$ V vs. Li^+/Li^0 . SSP compares favourably with TFSI, which has $\Delta E_v = 4.52$ V vs. Li^+/Li^0 .

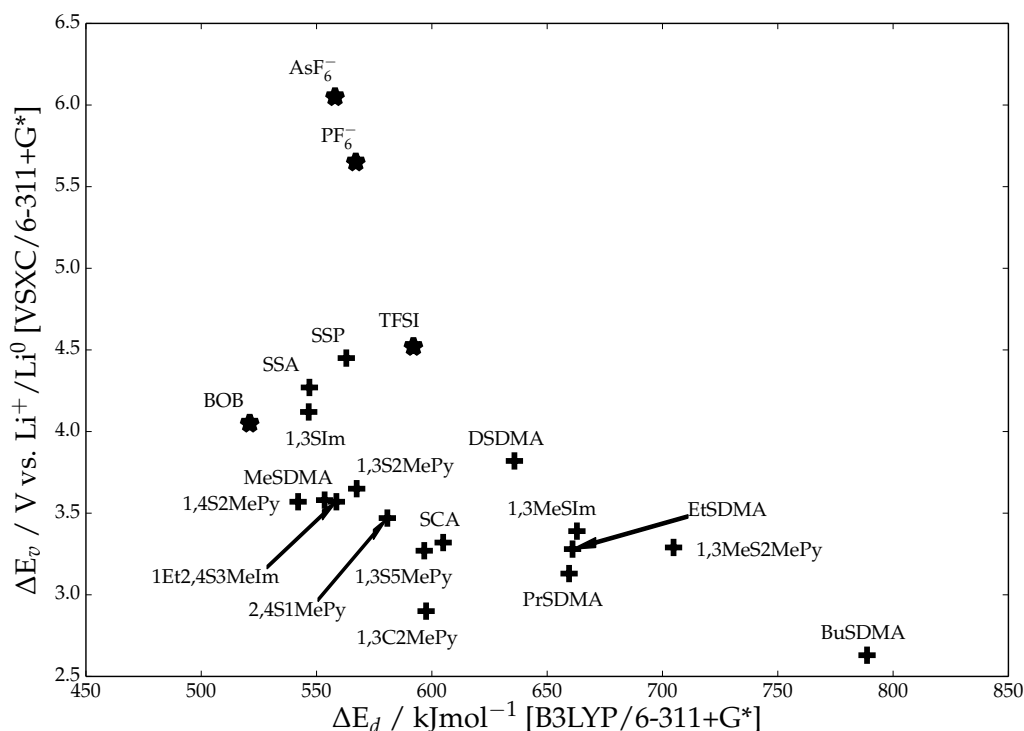


Figure 16: A Scheers plot of the pseudo-delocalized anions of Paper II along with reference anions.

For novel anions, the two emphasised properties are ΔE_v and ΔE_d , thus for the anions of Paper II, it is relevant to create a Scheers plot²⁷³ (Figure 16) to gauge the anion performance. Three of the pseudo-delocalized anions should, based on this, be prioritised for synthesis attempts; SSA, SSP and 1,3SIm. They all have both similar performance as BOB and TFSI electrochemically and have ΔE_d values that surpass or are on par with PF_6^- and AsF_6^- .

As previously mentioned, there are no clear E_{ox} reference values for comparison to benchmark the theoretical study of oxidation potentials. Therefore, to get a computational benchmark, a CCSD(T)/CBS study was designed (Paper V). This was possible for a number of small anions, while an alternative approach utilising an approximate CBS approach (described in Section 3.5.2), designated as ΔCBS , was used for larger anions.

This benchmark allows for the exploration of the application of new DFT functionals – leveraging the recently developed functionals, and validating previous functionals. The benchmarking revealed that a ΔE_v value calculated with a DFT functional will on average be too low. VSXC, the previously recommended functional for ΔE_v calculations, was found

to be the worst performing functional – though not poor enough to be concerning for prior results. Furthermore, either a hybrid or a double hybrid functional is recommended and M06-2X is recommended in particular.

An alternative approach was also assessed for the study of oxidation potentials, the anion hardness, η . It measures the resistance of the system against changes in the number of electrons. In Paper V it was implemented by a finite difference scheme, requiring single point calculations for both the reduced and oxidised radicals of the anion. As for the ΔE_v study, CBS and Δ CBS values were calculated for η , allowing for a benchmark.

η proved to compare favourably with the E_{ox} values and unlike the ΔE_v approach to get the correct ordering of the halide ions, *i.e.* $F^- > Cl^- > Br^-$, for all tested DFT functionals. Furthermore, the Δ CBS values showed that, on average, DFT functionals will slightly overestimate η . However, there were some exceptions that proved to be valid for all functionals, albeit differing in magnitude. Again double hybrid functionals receive a recommendation as does M06-2X. However, the relationship between η and E_{ox} is not clear, thus making it surprising to see that the η values are so close to the experimental values vs. Li^+/Li^0 .

4.4 Thermal stability

The thermal stability of electrolyte salts is a property still unknown how to be properly predicted from an *ab initio* perspective. In Paper I a method is developed and tested for thermal stability prediction by looking at the bond stability of anions. The approach is to use a geometry optimised anion and calculating multiple single point energies along a bond, *i.e.* stretching it (Figure 17). It could seem sufficient to calculate a single point energy at the equilibrium bond length and at a large separation of nuclei. However, that approach can lead to spurious results due to an artificial lowering of the latter energy (Figure 17 (b)). This likely arises from the multi-reference nature of the stretched bond.²⁷⁴ Therefore, a multistep approach was taken to see if such problems were present for each system and to get comparable results for different stretched bonds.

The resulting bond breaking energies, ΔE_b , give information on the bond liable to break first, *e.g.* the S–C bond of TFSI. The prediction is not the same for all methods applied, however, as HF predicts the S=O bond to break. This can be an artefact of the smaller basis set used in the HF calculations. When ΔE_b is compared with experimental data, it is not a good descriptor for the thermal stability as *e.g.* it predicts a higher stability for PF_6^- than for TFSI.

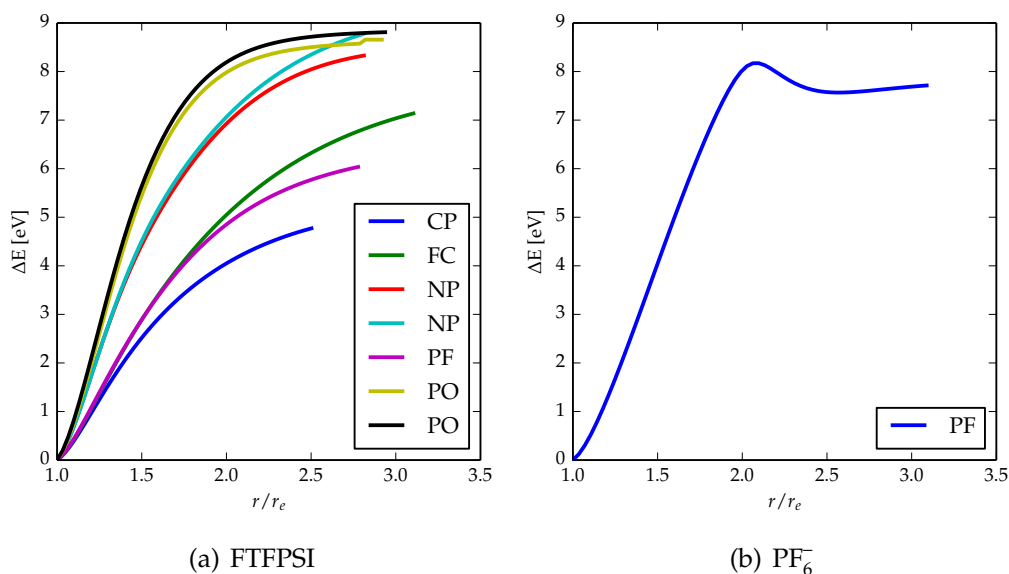


Figure 17: A demonstration of the bond breaking strategy applied to (a) FTFPSI and (b) PF_6^- , using UMP2/6-311+G(d). For the P–F bond of PF_6^- there is an artificial lowering of the energy at large r/r_e .

4.4.1 Bond breaking and recombination

An issue connected to thermal stability is decomposition and the resulting products. This is tackled in Paper VI in a combined experimental and computational study, where predicted products of decomposition are detected spectroscopically in a gas flow. In this paper, an algorithmic approach (described in Appendix A) is used to predict likely decomposition products to be detected, *i.e.* focusing on smaller neutral molecules, as the detection method is infrared (IR) spectroscopy of evolved gases from thermogravimetric analysis (TGA).

Two main systems were studied with this combined *ab initio*/experimental method; EMImTFSI and LiTFSI. For EMImTFSI it was possible to assign a large number of peaks, and thus identify some of the thermal decomposition products, some of which previously detected in the literature and others novel. For LiTFSI, fewer peaks were assignable, and in the spectra a number of peaks, in the $2000\text{ cm}^{-1} - 2500\text{ cm}^{-1}$ range, had no correspondence at all to the *ab initio* derived spectra, possibly implying a different decomposition mechanism for LiTFSI.

4.5 Localization

The pseudo-delocalized anions studied in PaperII all have an unusual structure due to the two negative moieties around a cationic core.

Starting from the definition of the anions, localizing electrons to certain parts of the molecule, would make it possible to see net charges of each moiety. Therefore a simple measure was designed from the formal charge of the cationic core being 1. If the anion is fully pseudo-delocalized, then this measure, the pseudo-delocalization measure, $\%_{pd}$, should give 100% or 1. If an anion has its charge fully delocalized over the entire molecule, then the cationic core should have a charge of $-1/3$. The pseudo-delocalization measure, $\%_{pd}$, is defined as:

$$\%_{pd} = \frac{\sum_{i_{\text{cationic}}} q_i + \frac{1}{3}}{1\frac{1}{3}} = (3\delta_+ + 1) / 4$$

where q_i is the charge of the individual atoms of the cationic core – thus δ_+ is the total charge of the cationic core. To localize the electrons to the atoms of the different moieties the program Bader was used, which implements AIM.^{246–248}

Chapter 5

Summary of Appended Papers

Paper I

In this paper novel imides are studied and the effect of the choices of functional group on their oxidative and thermal stability, and their ion-pair dissociation reaction with Li^+ . The anions are sulfonyl, $[\text{R}_1\text{SO}_2\text{NSO}_2\text{R}_2]^-$, and phosphoryl, $[(\text{R}_1)_2\text{P}=\text{ONP}=\text{O}(\text{R}_2)_2]^-$ imides (depicted in Figure 18). R_1 and R_2 can be one of the following functional groups: $-\text{F}$, $-\text{CF}_3$ and $-\text{C}\equiv\text{N}$.

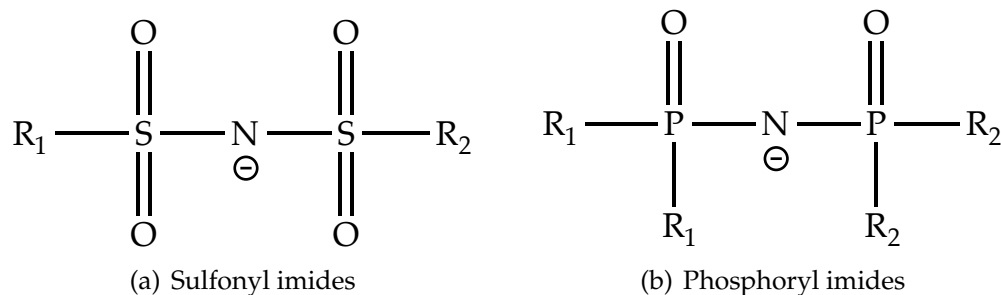


Figure 18: A number of imides, where R_1 and R_2 can be one of $-\text{F}$, $-\text{CF}_3$ and $-\text{C}\equiv\text{N}$.

The main result is a systematic effect, where the $-\text{C}\equiv\text{N}$ functional group decreases the ΔE_d value and increases the ΔE_v value. However, the thermal stability of the bonds seem to be inversely proportional to ΔE_d .

Paper II

Pseudo-delocalized anions is a new concept for anion design for lithium battery electrolytes (patent pending). They consist of a cationic core with at least two anionic moieties. As the charge of the anion is neither fully

localized to a single part nor fully delocalized, the anion is called a pseudo-delocalized anion. A schematic drawing of the concept is seen in Figure 19 along with an example.

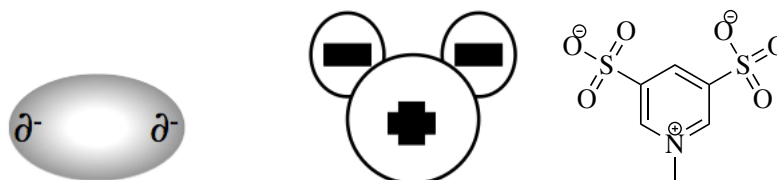


Figure 19: A schematic drawing of the pseudo-delocalized anion concept; left a conventional fully delocalized anion; middle a pseudo-delocalized anion; right 1,3-disulfonate-5-methyl-pyridine, one of the pseudo-delocalized anions – with a ΔE_d of $596.7 \text{ kJ mol}^{-1}$ and a ΔE_v of $3.27 \text{ V vs. Li}^+/\text{Li}^0$

All of the anions are verified to be pseudo-delocalized (by the measure discussed in Section 4.5), with some variation in the $\%_{pd}$ value. Additionally a similarly looking anion, $\text{Im}(\text{BF}_3)_2^-$ is verified not to be pseudo-delocalized.

Paper III

This paper studies the effect of replacing lithium with sodium. It is partly based on previous work where a large number of anions were studied to find their ion-pair dissociation energy.⁸¹ ΔE_d is used as a measure to explore the effect of replacing Li^+ with Na^+ .

This uniformly results in a decreased ΔE_d for sodium ion-pairs (as compared to the corresponding lithium ion-pairs). This effect is shown in Figure 20, where a trend of 20% reduction in ion-pair dissociation energy is seen. A few of the anions are particularly promising for further experimental studies aimed at sodium-ion batteries.

Paper IV

This paper looks in depth at the local solvation structures of both Li^+ and Na^+ using the common electrolyte solvents EC and DMC. A series of solvation structures were set up, from 2 to 8 solvent molecules, with all possible combinations of EC and DMC in common molecular symmetries (e.g. tetrahedral).

Both ΔE_{solv} and ΔE_{bind} (Section 4.2) are calculated for each structure. The subsequent analysis shows that DMC should play a role in the solvation of

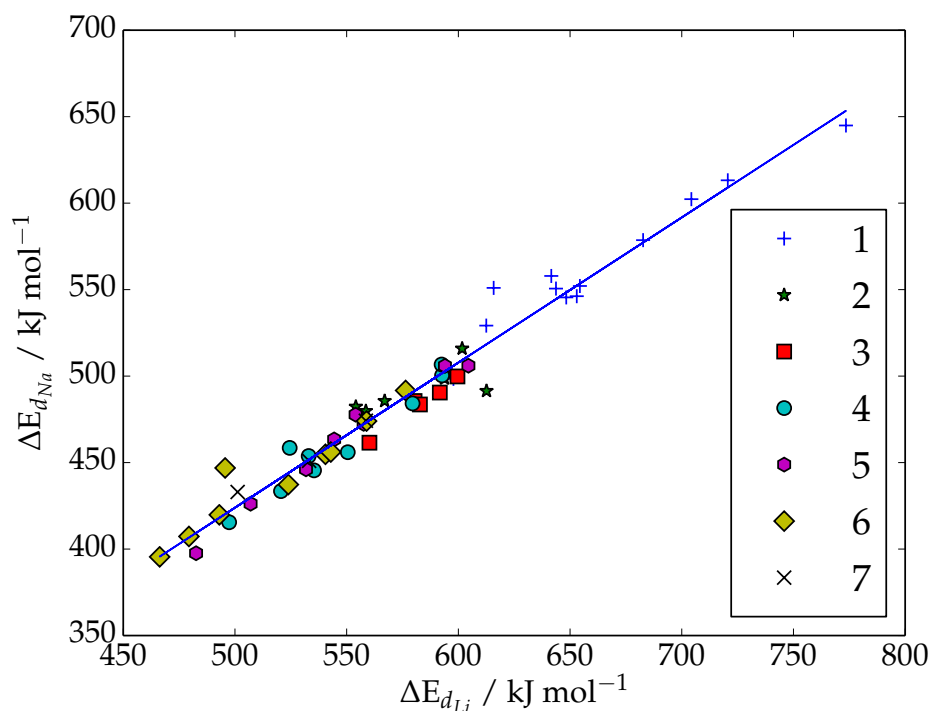


Figure 20: The ΔE_d of Li^+ and Na^+ as calculated with B3LYP/6-311+G*

the alkali cations, with the dominant structures being $\text{Li}(\text{EC})_2(\text{DMC})_2^+$ and $\text{Na}(\text{DMC})_4^+$.

As the software used for the initial high-throughput screening applied only the small 6-31G basis set; the dispersion corrected B3LYP functional is used to compensate for the small size of the basis set. To compensate both for the small basis set and to fully address the role of the conformational equilibrium of DMC, a series of structures are moved to high level calculations. The results obtained further emphasise the role DMC plays in the solvation of Li^+ and Na^+ and show the effect of the conformational equilibrium of DMC.

Paper V

In this paper oxidation potentials of benchmark quality are reported. Furthermore, the performance of a number of DFT functionals is studied, finding that for ΔE_v calculations, a hybrid or higher level DFT functional is recommended.

A different measure for the oxidation potential is also explored in the

paper, the hardness η , which is found to correlate nicely with experimental values. Hardness values of benchmark quality were also reported along with a comparison of DFT functional performance.

Paper VI

The thermal decomposition products of an IL, EMImTFSI, and a salt, LiTFSI, are predicted with *ab initio* methods. The predictions are combined with TGA/IR measurements, where *ab initio* derived spectra are used to identify peaks in IR spectra, thus identifying decomposition products.

Paper VII

This is an experimental study, employing Raman spectroscopy – a follow up to Paper IV. Here the prediction of Paper IV is confirmed, *i.e.* DMC is a part of the solvation shell around Li^+ in EC/DMC solvent mixtures. Furthermore, it also shows that to get the full picture of the solvation contribution of DMC, a second Raman peak, due to the DMC cis-cis conformer, must be analysed.

Chapter 6

Conclusion and Outlook

In this thesis a number of *ab initio* methods have been employed to aid in the understanding and possible improvement of electrolytes for LIBs. Furthermore, to help with the rapid development of SIBs, same research was performed concurrently. The key results are:

- A number of novel anions, pseudo-delocalized anions, are shown to be promising for future applications in lithium and/or sodium batteries. These anions have the benefit of being fluorine free, a dual safety and cost feature.
- The thermal stability of anions is studied with a new approach, utilising stretched bonds, though with limited success. The thermal decomposition products are also predicted (with an algorithmic approach) and a subset of the products are confirmed by experiments.
- There are predictions of the local environment of lithium and sodium cations in the common carbonate solvents, EC and DMC. For lithium, they are in agreement with some experimental studies, while for sodium there is no direct experimental comparison yet to be made. These are followed up by experiments that support the conclusion of the computational paper.
- The properties of the sodium salts seem to be amenable in the same manner as lithium salts, via the prediction of their ion-pair dissociation energy ΔE_d . As there is a strong trend for sodium salts to give 20% lower ΔE_d , one would expect the sodium salts to have improved conductivity compared to their lithium counterparts. However, due to the concurrent drop in solvation energy, that results in a status quo. On a more positive note, this reveals that the know-how in the

LIB electrolyte field will be for most part transferrable over to SIB electrolytes, resulting in a synergy for LIB and SIB development.

- Another aspect of battery electrolytes studied is their stability vs. oxidation. Unfortunately, there is a dearth of systematic experimental studies which allow for a straightforward comparison of all reported lithium salts in the literature. Thus a high level theory approach was used to get benchmark values for oxidation potentials. This allowed for a study of DFT functional performance which showed that at least hybrid functionals are recommended. Furthermore, a different measure, the anions' hardness, is tested for its application in prediction oxidation stability – which is shown to perform well.

The LIB is here to stay, but its counterpart the SIB is just around the corner, which may applications in different fields. How they will be used is still an open question, which will only answered once SIBs are commercialised – as none predicted the mobile computing industry, partly if not entirely made possible by LIBs.

To get further in this field, more collaborations between those wielding *ab initio* methods and those doing measurements can result in fruitful work as they can back each other up, as seen with Papers VI and VII. This can be in either direction as Paper VII complements the *ab initio* results of Paper IV and in Paper VI aimed at supporting measurements by helping with interpretation.

In this age of Big Data, the thermal decomposition seems to be a problem that will be amenable to in depth data analysis. While it is a complicated problem, as a combinatorial analysis of the possible structural variations would show, the power of algorithmic approaches is remarkable and could possibly allow for the identification of all the reaction products. Then it might be possible to backtrack what all of the breakdown reaction are.

Acknowledgements

I would like to start by thanking my supervisor, Patrik Johansson, for the freedom, the encouragements and the resources I have had in my work. He also pushed me to not just do science, but to excel, even though the cost was a river of red ink. I also thank the great support I have had in the KMF group, both from former and current members. Some people I must mention separately, such as Johan Sc. and Jagath for the many great discussions we have had. Aleks for taking over as main co-supervisor. Other people that I must mention are Johan B., Susanne, Pelle and Luis.

Not everyone that I have collaborated with have been at Chalmers, so I must thank Michel Armand for his role in my first project here in Sweden! Then there is also the group of Wesley Henderson, where I have only met some of them, then after more than a year of collaboration.

Additionally, funding from the Swedish Energy Agency via a VR/STEM grant is acknowledged and the allocation of computational resources from SNIC. There have also been generous travel grants from Ångpanneföreningens Forskningsstiftelse for IMLB in Jeju, South Korea and from Svenska Kemistsamfundet for ISPE in Selfoss, Iceland.

Ég vil þakka fjölskyldunni minni og vinum fyrir að hafa stutt við mig í þessu námi. Ég vil einnig þakka þessa fyrir að fá mig til að skoða heimasíðu Chalmers einn örlagaríkan dag í maí – það endaði sem doktorsnám í Svíþjóð, þó ég hafi verið skammaður fyrir tölvuhangs í afmæli.

And for Per:

En orðstír

deyr aldregi

hveim er sér góðan getur.

Bibliography

- [1] Tarascon, J. M.; Armand, M. *Nature* **2001**, *414*, 359–367.
- [2] Dagenborg, J. *Reuters* – Tesla’s Model S overtakes VW Golf as Norway’s best-selling car – Oct 8, 2013. <http://www.reuters.com/article/2013/10/08/tesla-norway-idUSL6N0HX1CH20131008>.
- [3] Yang, Z.; Zhang, J.; Kintner-Meyer, M. C. W.; Lu, X.; Choi, D.; Lemmon, J. P.; Liu, J. *Chem. Rev.* **2011**, *111*, 3577–3613.
- [4] (a) Slater, M. D.; Kim, D.; Lee, E.; Johnson, C. S. *Adv. Funct. Mater.* **2012**, *23*, 947–958; (b) Slater, M. D.; Kim, D.; Lee, E.; Doeff, M.; Johnson, C. S. *Adv. Funct. Mater.* **2012**, *23*, 3255.
- [5] Tarascon, J.-M. *Nat. Chem.* **2010**, *2*, 510.
- [6] Thomas, P.; Ghanbaja, J.; Billaud, D. *Electrochim. Acta* **1999**, *45*, 423–430.
- [7] Ding, J. et al. *ACS Nano* **2013**, *7*, 11004–11015.
- [8] Jacoby, M. *Chem. Eng. News* **2013**, *91*, 33–37.
- [9] Watt, A.; Philip, A. *The electro-plating and electro-refining of metals: being a new ed. of Alexander Watt’s “Electro-deposition”*; C. Lockwood and Son, 1902.
- [10] Palacín, M. R. *Chem. Soc. Rev.* **2009**, *38*, 2565–2575.
- [11] Jayaprakash, N.; Das, S. K.; Archer, L. A. *Chem. Commun.* **2011**, *47*, 12610–12612.
- [12] Yoo, H. D.; Shterenberg, I.; Gofer, Y.; Gershinshy, G.; Pour, N.; Aurbach, D. *Energy Environ. Sci.* **2013**, *6*, 2265–2279.
- [13] Pan, H.; Hu, Y.-S.; Chen, L. *Energy Environ. Sci.* **2013**, *6*, 2338–2360.
- [14] Bratsch, S. G. *J. Phys. Chem. Ref. Data* **1989**, *18*, 1–21.
- [15] Scrosati, B.; Selvaggi, A.; Croce, F.; Gang, W. J. *Power Sources* **1988**, *24*, 287–294.

- [16] Sawai, K.; Iwakoshi, Y.; Ohzuku, T. *Solid State Ionics* **1994**, *69*, 273–283.
- [17] Ozawa, K. *Solid State Ionics* **1994**, *69*, 212–221.
- [18] Scrosati, B. J. *Electrochem. Soc.* **1992**, *139*, 2776–2781.
- [19] Wilken, S.; Johansson, P.; Jacobsson, P. In *Lithium Batteries Advanced Technologies and Applications*; Scrosati, B., Abraham, K. M., van Schalkwijk, W., Hassoun, J., Eds.; John Wiley & Sons, Inc.: Hoboken, New Jersey, 2013; pp 39–70.
- [20] Abraham, K. M.; Pasquariello, D. M.; Willstaedt, E. B. J. *Electrochem. Soc.* **1990**, *137*, 1856–1857.
- [21] Narayanan, S. R.; Surampudi, S.; Attia, A. I.; Bankston, C. P. J. *Electrochem. Soc.* **1991**, *138*, 2224–2229.
- [22] Han, Y.-K.; Jung, J.; Yu, S.; Lee, H. J. *Power Sources* **2009**, *187*, 581–585.
- [23] Zhang, S. S. J. *Power Sources* **2006**, *162*, 1379–1394.
- [24] Arora, P.; Zhang, Z. J. *Chem. Rev.* **2004**, *104*, 4419–4462.
- [25] Goodenough, J. B.; Kim, Y. J. *Power Sources* **2011**, *196*, 6688–6694.
- [26] Goodenough, J. B.; Park, K.-S. J. *Am. Chem. Soc.* **2013**, *135*, 1167–1176.
- [27] Marom, R.; Amalraj, S. F.; Leifer, N.; Jacob, D.; Aurbach, D. J. *Mater. Chem.* **2011**, *21*, 9938.
- [28] Huggins, R. A. *Advanced Batteries: Materials Science Aspects*; Springer: New York, 2009.
- [29] Daniel, C., Besenhard, J. O., Eds. *Handbook of Battery Materials*, 2nd ed.; Wiley-VCH, 2011.
- [30] Mohri, M.; Yanagisawa, N.; Tajima, Y.; Tanaka, H.; Mitate, T.; Nakajima, S.; Yoshida, M.; Yoshimoto, Y.; Suzuki, T.; Wada, H. J. *Power Sources* **1989**, *26*, 545–551.
- [31] Peled, E. J. *Electrochem. Soc.* **1979**, *126*, 2047–2051.
- [32] Fong, R.; von Sacken, U.; Dahn, J. R. J. *Electrochem. Soc.* **1990**, *137*, 2009–2013.
- [33] Xu, K. J. *Electrochem. Soc.* **2009**, *156*, A751–A755.
- [34] Wang, Y.; Nakamura, S.; Ue, M.; Balbuena, P. B. J. *Am. Chem. Soc.* **2001**, *123*, 11708–11718.

- [35] Wang, Y.; Balbuena, P. B. *Int. J. Quantum Chem.* **2005**, *102*, 724–733.
- [36] Xu, K.; Lam, Y.; Zhang, S. S.; Jow, T. R.; Curtis, T. B. *J. Phys. Chem. C* **2007**, *111*, 7411–7421.
- [37] Gachot, G.; Grugeon, S.; Armand, M.; Pilard, S.; Guenot, P.; Tarascon, J.-M.; Laruelle, S. *J. Power Sources* **2008**, *178*, 409–421.
- [38] Bhattacharyya, R.; Key, B.; Chen, H.; Best, A. S.; Hollenkamp, A. F.; Grey, C. P. *Nat. Mat.* **2010**, *9*, 504–510.
- [39] Kim, S.-P.; van Duin, A. C. T.; Shenoy, V. B. *J. Power Sources* **2011**, *196*, 8590–8597.
- [40] Chandrashekar, S.; Trease, N. M.; Chang, H. J.; Du, L.-S.; Grey, C. P.; Jerschow, A. *Nat. Mat.* **2012**, *11*, 311–315.
- [41] Shkrob, I. A.; Zhu, Y.; Marin, T. W.; Abraham, D. *J. Phys. Chem. C* **2013**, 19255–19269.
- [42] Shkrob, I. A.; Zhu, Y.; Marin, T. W.; Abraham, D. *J. Phys. Chem. C* **2013**, 19270–19279.
- [43] Onuki, M.; Kinoshita, S.; Sakata, Y.; Yanagidate, M.; Otake, Y.; Ue, M.; Deguchi, M. *J. Electrochem. Soc.* **2008**, *155*, A794–A797.
- [44] Leifer, N.; Smart, M. C.; Prakash, G. K. S.; Gonzalez, L.; Sanchez, L.; Smith, K. A.; Bhalla, P.; Grey, C. P.; Greenbaum, S. G. *J. Electrochem. Soc.* **2011**, *158*, A471–A480.
- [45] Colbow, K. M.; Dahn, J. R.; Haering, R. R. *J. Power Sources* **1989**, *26*, 397–502.
- [46] Whittingham, M. S. *Chem. Rev.* **2004**, *104*, 4271–4302.
- [47] Whittingham, M. S. *Science* **1976**, *192*, 1126–1127.
- [48] Mizushima, K.; Jones, P. C.; Wiseman, P. J.; Goodenough, J. B. *Mat. Res. Bull.* **1980**, *15*, 783–789.
- [49] Thackeray, M. M.; David, W. I. F.; Bruce, P. G.; Goodenough, J. B. *Mat. Res. Bull.* **1983**, *18*, 461–472.
- [50] Padhi, A. K.; Nanjundaswamy, K. S.; Goodenough, J. B. *J. Electrochem. Soc.* **1997**, *144*, 1188–1194.
- [51] Fletcher, S. *Bottled Lightning: Superbatteries, Electric Cars, And The New Lithium Economy*; Hill and Wang: New York, 2011.

- [52] Barker, J.; Saidi, M. Y.; Swoyer, J. L. *J. Electrochem. Soc.* **2003**, *150*, A1394.
- [53] Zaghbi, K.; Mauger, A.; Groult, H.; Goodenough, J.; Julien, C. *Materials* **2013**, *6*, 1028–1049.
- [54] Julien, C. M.; Mauger, A. *Ionics* **2013**, *19*, 951–988.
- [55] Kraysberg, A.; Ein-Eli, Y. *Adv. Energy Mater.* **2012**, *2*, 922–939.
- [56] Hu, M.; Pang, X.; Zhou, Z. *J. Power Sources* **2013**, *237*, 229–242.
- [57] Park, M.; Zhang, X.; Chung, M.; Less, G. B.; Sastry, A. M. *J. Power Sources* **2010**, *195*, 7904–7929.
- [58] Gores, H. J.; Barthel, J.; Zugmann, S.; Mossbauer, D.; Amereller, M.; Hartl, R.; Maurer, A. In *Handbook of Battery Materials*; Daniel, C., Besenhard, J. O., Eds.; Wiley-VCH: Weinheim, 2011; pp 525–626.
- [59] Gray, F.; Armand, M. In *Handbook of Battery Materials*; Daniel, C., Besenhard, J. O., Eds.; Wiley-VCH: Weinheim, 2011; pp 627–656.
- [60] Baril, D.; Michot, C.; Armand, M. *Solid State Ionics* **1997**, *94*, 35–47.
- [61] Ong, S. P.; Andreussi, O.; Wu, Y.; Marzari, N.; Ceder, G. *Chem. Mater.* **2011**, *23*, 2979–2986.
- [62] Howlett, P. C.; Izgorodina, E. I.; Forsyth, M.; MacFarlane, D. R. *Z. Phys. Chem.* **2006**, *220*, 1483–1498.
- [63] Markevich, E.; Sharabi, R.; Borgel, V.; Gottlieb, H.; Salitra, G.; Aurbach, D.; Semrau, G.; Schmidt, M. A. *Electrochim. Acta* **2010**, *55*, 2687–2696.
- [64] (a) Johansson, P. *J. Phys. Chem. A* **2006**, *110*, 12077–12080; (b) Johansson, P. *J. Phys. Chem. A* **2007**, *111*, 1378–1379.
- [65] Zhang, S. S. *Electrochem. Commun.* **2006**, *8*, 1423–1428.
- [66] Sloop, S. E.; Pugh, J. K.; Wang, S.; Kerr, J. B.; Kinoshita, K. *Electrochem. Solid St.* **2001**, *4*, A42–A44.
- [67] Archuleta, M. M. *J. Power Sources* **1995**, *54*, 138–142.
- [68] Xu, K. *Chem. Rev.* **2004**, *104*, 4303–4418.
- [69] Xu, K.; von Cresce, A. *J. Mater. Chem.* **2011**, *21*, 9849–9864.
- [70] Kita, F.; Kawakami, A.; Nie, J.; Sonoda, T.; Kobayashi, H. *J. Power Sources* **1997**, *68*, 307–310.

- [71] Xu, W.; Angell, C. A. *Electrochem. Solid-State Lett.* **2001**, *4*, E1–E4.
- [72] Xu, K.; Zhang, S. S.; Lee, U.; Allen, J. L.; Jow, T. R. *J. Power Sources* **2005**, *146*, 79–85.
- [73] Zhang, X.; Devine, T. M. *J. Electrochem. Soc.* **2006**, *153*, B365–B369.
- [74] Xu, K.; Zhang, S.; Jow, R. *J. Power Sources* **2005**, *143*, 197–202.
- [75] Ding, M. S.; Richard Jow, T. *J. Electrochem. Soc.* **2004**, *151*, A2007–A2015.
- [76] Ue, M.; Takeda, M.; Takehara, M.; Mori, S. *J. Electrochem. Soc.* **1997**, *133*, 2684–2688.
- [77] Schmidt, M.; Heider, U.; Kuehner, A.; Oesten, R.; Jungnitz, M.; Ignat'ev, N.; Sartori, P. *J. Power Sources* **2001**, *97-98*, 557–560.
- [78] Wilken, S.; Johansson, P.; Jacobsson, P. *Solid State Ionics* **2012**, *225*, 608–610.
- [79] Barthel, J.; Buestrich, R.; Carl, E.; Gores, H. J. *J. Electrochem. Soc.* **1996**, *143*, 3572–3575.
- [80] Barthel, J.; Gores, H.; Neueder, R.; Schmid, A. *Pure Appl. Chem.* **1999**, *71*, 1705–1715.
- [81] Johansson, P. *Phys. Chem. Chem. Phys.* **2007**, *9*, 1493–1498.
- [82] Jónsson, E.; Armand, M.; Johansson, P. *Phys. Chem. Chem. Phys.* **2012**, *14*, 6021–6025.
- [83] Abouimrane, A.; Ding, J.; Davidson, I. J. *J. Power Sources* **2009**, *189*, 693–696.
- [84] Han, H.-B. et al. *J. Power Sources* **2011**, *196*, 3623–3632.
- [85] (a) Scheers, J.; Jónsson, E.; Jacobsson, P.; Johansson, P. *Electrochemistry* **2012**, *80*, 18–25; (b) Scheers, J.; Jónsson, E.; Jacobsson, P.; Johansson, P. *Electrochemistry* **2012**, *80*, 142.
- [86] Murmann, P.; Niehoff, P.; Schmitz, R.; Nowak, S.; Gores, H.; Ignatiev, N.; Sartori, P.; Winter, M.; Schmitz, R. *Electrochim. Acta* **2013**, *114*, 658–666.
- [87] Barthel, J.; Wühr, M.; Buestrich, R.; Gores, H. J. *J. Electrochem. Soc.* **1995**, *142*, 2527–2531.
- [88] Barthel, J.; Buestrich, R.; Carl, E.; Gores, H. J. *J. Electrochem. Soc.* **1996**, *143*, 3565–3571.
- [89] Barthel, J.; Buestrich, R.; Gores, H.; Schmidt, M.; Wühr, M. *J. Electrochem. Soc.* **1997**, *144*, 3866–3870.

- [90] Barthel, J.; Schmidt, M.; Gores, H. J. *J. Electrochem. Soc.* **1998**, *145*, L17–L20.
- [91] Barthel, J.; Schmid, A.; Gores, H. J. *J. Electrochem. Soc.* **2000**, *147*, 21–24.
- [92] Kaymaksiz, S.; Wilhelm, F.; Wachtler, M.; Wohlfahrt-Mehrens, M.; Hartnig, C.; Tschernych, I.; Wietelmann, U. *J. Power Sources* **2013**, *239*, 659–669.
- [93] Xu, W.; Angell, C. A. *Electrochem. Solid-State Lett.* **2000**, *3*, 366–368.
- [94] Xu, K.; Zhang, S.; Poese, B. A.; Jow, T. R. *Electrochem. Solid-State Lett.* **2002**, *5*, A259–A262.
- [95] Yamaguchi, H.; Takahashi, H.; Kato, M.; Arai, J. *J. Electrochem. Soc.* **2003**, *150*, A312–A315.
- [96] Xu, W.; Shusterman, A. J.; Marzke, R.; Angell, C. A. *J. Electrochem. Soc.* **2004**, *151*, A632–A638.
- [97] Zugmann, S. et al. *J. Power Sources* **2011**, *196*, 1417–1424.
- [98] Chen, Z.; Liu, J.; Amine, K. *Electrochem. Solid-State Lett.* **2007**, *10*, A45–A47.
- [99] Kita, F.; Sakata, H.; Kawakami, A.; Kamizori, H.; Sonoda, T.; Nagashima, H.; Pavlenko, N. V.; Yagupolskii, Y. L. *J. Power Sources* **2001**, *97–98*, 581–583.
- [100] Wietelmann, U.; Bonrath, W.; Netscher, T.; Nöth, H.; Panitz, J.-C.; Wohlfahrt-Mehrens, M. *Chem. Eur. J.* **2004**, *10*, 2451–2458.
- [101] Handa, M.; Suzuki, M.; Suzuki, J.; Kanematsu, H.; Sasaki, Y. *Electrochem. Solid-State Lett.* **1999**, *2*, 60–62.
- [102] Xu, M.; Xiao, A.; Li, W.; Lucht, B. L. *Electrochem. Solid-State Lett.* **2009**, *12*, A155–A158.
- [103] Xiao, A.; Yang, L.; Lucht, B. L. *Electrochem. Solid-State Lett.* **2007**, *10*, A241–A244.
- [104] Johansson, P.; Béranger, S.; Armand, M.; Nilsson, H.; Jacobsson, P. *Solid State Ionics* **2003**, *156*, 129–139.
- [105] Niedzicki, L.; Kasprzyk, M.; Kuziak, K.; Żukowska, G. Z.; Armand, M.; Bukowska, M.; Marcinek, M.; Szczeciński, P.; Wieczorek, W. *J. Power Sources* **2009**, *192*, 612–617.
- [106] Niedzicki, L. et al. *Electrochim. Acta* **2010**, *55*, 1450–1454.
- [107] Niedzicki, L.; Kasprzyk, M.; Kuziak, K.; Żukowska, G. Z.; Marcinek, M.; Wieczorek, W.; Armand, M. *J. Power Sources* **2011**, *196*, 1386–1391.

- [108] Barbarich, T. J.; Driscoll, P. F. *Electrochem. Solid-State Lett.* **2003**, *6*, A113–A116.
- [109] Barbarich, T. J.; Driscoll, P. F.; Izquierdo, S.; Zakharov, L. N.; Incarvito, C. D.; Rheingold, A. L. *Inorg. Chem.* **2004**, *43*, 7764–7773.
- [110] Ivanova, S. M.; Nolan, B. G.; Kobayashi, Y.; Miller, S. M.; Anderson, O. P.; Strauss, S. H. *Chem. Eur. J.* **2001**, *7*, 503–510.
- [111] Xue, Z.-M.; Wu, K.-N.; Liu, B.; Chen, C.-H. *J. Power Sources* **2007**, *171*, 944–947.
- [112] Scheers, J.; Johansson, P.; Jacobsson, P. J. *Electrochem. Soc.* **2008**, *155*, A628–A634.
- [113] Matsuda, Y.; Fukushima, T.; Hashimoto, H.; Arakawa, R. J. *Electrochem. Soc.* **2002**, *149*, A1045–A1048.
- [114] von Cresce, A.; Xu, K. *Electrochem. Solid-State Lett.* **2011**, *14*, A154–A156.
- [115] Jeong, S.-K.; Inaba, M.; Iriyama, Y.; Abe, T.; Ogumi, Z. *Electrochim. Acta* **2002**, *47*, 1975–1982.
- [116] Morita, M.; Asai, Y.; Yoshimoto, N.; Ishikawa, M. *Faraday Trans.* **1998**, *94*, 3451–3456.
- [117] Ikezawa, Y.; Nishi, H. *Electrochim. Acta* **2008**, *53*, 3663–3669.
- [118] Borodin, O.; Smith, G. D. *J. Phys. Chem. B* **2009**, *113*, 1763–1776.
- [119] Castriota, M.; Cazzanelli, E.; Nicotera, I.; Coppola, L.; Oliviero, C.; Ranieri, G. A. *J. Chem. Phys.* **2003**, *118*, 5537–5541.
- [120] Cazzanelli, E.; Mustarelli, P.; Benevelli, F.; Appetecchi, G. B.; Croce, F. *Solid State Ionics* **1996**, *86-88*, 379–384.
- [121] Bogle, X.; Vazquez, R.; Greenbaum, S.; Cresce, A. v. W.; Xu, K. *J. Phys. Chem. Lett.* **2013**, *4*, 1664–1668.
- [122] Postupna, O. O.; Kolesnik, Y. V.; Kalugin, O. N.; Prezhdo, O. V. *J. Phys. Chem. B* **2011**, *115*, 14563–14571.
- [123] Chen, X.; Usrey, M.; Peña-Hueso, A.; West, R.; Hamers, R. J. *J. Power Sources* **2013**, *241*, 311–319.
- [124] Xu, K.; Angell, C. A. *J. Electrochem. Soc.* **1998**, *145*, L70–L72.
- [125] Oesten, R.; Heider, U.; Schmidt, M. *Solid State Ionics* **2002**, *148*, 391–397.
- [126] Aurbach, D.; K, G.; Markovsky, B.; Gofer, Y.; Schmidt, M.; Heider, U. *Electrochim. Acta* **2002**, *47*, 1423–1439.

- [127] Qin, Y.; Chen, Z.; Liu, J.; Amine, K. *Electrochem. Solid St.* **2010**, *13*, A11–A14.
- [128] Binnemans, K. *Chem. Rev.* **2007**, *107*, 2592–2614.
- [129] Armand, M.; Endres, F.; MacFarlane, D. R.; Ohno, H.; Scrosati, B. *Nat. Mat.* **2009**, *8*, 621–629.
- [130] Lewandowski, A.; Świdarska-Mocek, A. *J. Power Sources* **2009**, *194*, 601–609.
- [131] Forgie, J. C.; El Khakani, S.; MacNeil, D. D.; Rochefort, D. *Phys. Chem. Chem. Phys.* **2013**, *15*, 7713–7721.
- [132] Forgie, J. C.; Rochefort, D. *RSC Adv.* **2013**, *3*, 12035–12038.
- [133] *Mineral Commodity Summaries 2011*; U.S. Geological Survey, 2011.
- [134] Lu, X.; Xia, G.; Lemmon, J. P.; Yang, Z. *J. Power Sources* **2010**, *195*, 2431–2442.
- [135] Sudworth, J. L. *J. Power Sources* **2001**, *100*, 149–163.
- [136] Whittingham, M. S. *Prog. Solid. St. Chem.* **1978**, *12*, 41–99.
- [137] Stevens, D. A.; Dahn, J. R. *J. Electrochem. Soc.* **2000**, *147*, 1271–1273.
- [138] Alcántara, R.; Lavela, P.; Ortiz, G. F.; Tirado, J. L. *Electrochem. Solid-State Lett.* **2005**, *8*, A222–A225.
- [139] Chevrier, V. L.; Ceder, G. *J. Electrochem. Soc.* **2011**, *158*, A1011–A1014.
- [140] Senguttuvan, P.; Rouse, G.; Seznec, V.; Tarascon, J.-M.; Palacín, M. R. *Chem. Mater.* **2011**, *23*, 4109–4111.
- [141] Barker, J.; Saidi, M.; Swoyer, J. *Electrochem. Solid-State Lett.* **2003**, *6*, A1–A4.
- [142] Islam, M. S.; Dominko, R.; Masquelier, C.; Sirisopanaporn, C.; Armstrong, A. R.; Bruce, P. G. *J. Mater. Chem.* **2011**, *21*, 9811–9818.
- [143] Ong, S. P.; Chevrier, V. L.; Hautier, G.; Jain, A.; Moore, C.; Kim, S.; Ma, X.; Ceder, G. *Energy Environ. Sci.* **2011**, *4*, 3680–3688.
- [144] Hong, S. Y.; Kim, Y.; Park, Y.; Choi, A.; Choi, N.-S.; Lee, K. T. *Energy Environ. Sci.* **2013**, *6*, 2067–2081.
- [145] Vidal-Abarca, C.; Lavela, P.; Tirado, J. L.; Chadwick, A. V.; Alfredsson, M.; Kelder, E. *J. Power Sources* **2012**, *197*, 314–318.
- [146] Egashira, M.; Asai, T.; Yoshimoto, N.; Morita, M. *Electrochimica Acta* **2011**, *58*, 95–98.

- [147] Ponrouch, A.; Marchante, E.; Courty, M.; Tarascon, J.-M.; Palacín, M. R. *Energy Environ. Sci.* **2012**, *5*, 8572–8583.
- [148] Ponrouch, A.; Dedryvère, R.; Monti, D.; Demet, A. E.; Ateba Mba, J. M.; Croguennec, L.; Masquelier, C.; Johansson, P.; Palacín, M. R. *Energy Environ. Sci.* **2013**, *6*, 2361–2369.
- [149] Noor, S. A. M.; Howlett, P. C.; MacFarlane, D. R.; Forsyth, M. *Electrochim. Acta* **2013**, *114*, 766–771.
- [150] Ahuja, R.; Blomqvist, A.; Larsson, P.; Pyykkö, P.; Zaleski-Ejgierd, P. *Phys. Rev. Lett.* **2011**, *106*, 018301.
- [151] Zaleski-Ejgierd, P.; Pyykkö, P. *Phys. Chem. Chem. Phys.* **2011**, *13*, 16510–16512.
- [152] Ceder, G.; Van der Ven, A. *Electrochim. Acta* **1999**, *45*, 131–150.
- [153] Hautier, G.; Jain, A.; Ong, S. P.; Kang, B.; Moore, C.; Doe, R.; Ceder, G. *Chem. Mater.* **2011**, *23*, 3495–3508.
- [154] Johansson, P.; Jacobsson, P. *Electrochim. Acta* **2001**, *46*, 1545–1552.
- [155] Johansson, P.; Nilsson, H.; Jacobsson, P.; Armand, M. *Phys. Chem. Chem. Phys.* **2004**, *6*, 895–899.
- [156] Scheers, J.; Niedzicki, L.; Żukowska, G. Z.; Johansson, P.; Wieczorek, W.; Jacobsson, P. *Phys. Chem. Chem. Phys.* **2011**, *13*, 11136–11147.
- [157] Herstedt, M.; Smirnov, M.; Johansson, P.; Chami, M.; Grondin, J.; Servant, L.; Lassègues, J. C. *J. Raman Spectrosc.* **2005**, *36*, 762–770.
- [158] Xing, L.; Vatamanu, J.; Borodin, O.; Smith, G. D.; Bedrov, D. J. *Phys. Chem. C* **2012**, *116*, 23871–23881.
- [159] Tasaki, K.; Kanda, K.; Nakamura, S.; Ue, M. *J. Electrochem. Soc.* **2003**, *150*, A1628–A1636.
- [160] Scheers, J.; Johansson, P. *J. Electrochem. Soc.* **2012**, *159*, A1–A2.
- [161] Li, L.; Zhou, S.; Han, H.; Li, H.; Nie, J.; Armand, M.; Zhou, Z.; Huang, X. *J. Electrochem. Soc.* **2011**, *158*, A74–A82.
- [162] Izgorodina, E. I. *Phys. Chem. Chem. Phys.* **2011**, *13*, 4189–4207.
- [163] Grimme, S.; Hujo, W.; Kirchner, B. *Phys. Chem. Chem. Phys.* **2012**, *14*, 4875–4883.

- [164] Zahn, S.; MacFarlane, D. R.; Izgorodina, E. I. *Phys. Chem. Chem. Phys.* **2013**, *15*, 13664–13675.
- [165] Angenendt, K.; Johansson, P. J. *Phys. Chem. B* **2011**, *115*, 7808–7813.
- [166] Tian, Y.-H.; Goff, G. S.; Runde, W. H.; Batista, E. R. *J. Phys. Chem. B* **2012**, *116*, 11943–11952.
- [167] Atkins, P.; Friedman, R. *Molecular Quantum Mechanics*, 4th ed.; Oxford University Press: Oxford, 2007.
- [168] Szabo, A.; Ostlund, N. S. *Modern Quantum Chemistry; Introduction to Advanced Electronic Structure Theory*; Dover Publications: Mineola, 1996.
- [169] Helgaker, T.; Jørgensen, P.; Olsen, J. *Molecular Electronic-Structure Theory*; Wiley: Chichester, 2012.
- [170] Cook, D. B. *Handbook of Computational Quantum Chemistry*; Dover books on chemistry; Dover Publications, 2005.
- [171] Garand, E.; Zhou, J.; Manolopoulos, D. E.; Alexander, M. H.; Neumark, D. M. *Science* **2008**, *319*, 72–75.
- [172] Bowman, J. M. *Science* **2008**, *319*, 40–41.
- [173] Gill, P. M. W. *Encyclopedia of Computational Chemistry*; Wiley: Chichester, 1998; pp 678–689.
- [174] Boys, S. F. *Proc. Roy. Soc.* **1950**, *A200*, 542–554.
- [175] Hehre, W. J.; Stewart, R. F.; Pople, J. A. *J. Chem. Phys.* **1969**, *51*, 2657–2664.
- [176] Ditchfield, R.; Hehre, W. J.; Pople, J. A. *J. Chem. Phys.* **1971**, *54*, 724–728.
- [177] Hehre, W.; Ditchfield, R.; Pople, J. A. *J. Chem. Phys.* **1972**, *56*, 2257–2261.
- [178] Chandrasekhar, J.; Andrade, J. G.; von Rague Schleyer, P. J. *Am. Chem. Soc.* **1981**, *103*, 5609–5612.
- [179] Clark, T.; Chandrasekhar, J.; Spitznagel, G. W.; Schleyer, P. V. R. *J. Comput. Chem.* **1983**, *4*, 294–301.
- [180] Hariharan, P.; Pople, J. *Theor. Chim. Acta* **1973**, *28*, 213–222.
- [181] Jensen, F. *WIREs Comput. Mol. Sci.* **2012**, *3*, 273–295.
- [182] Dunning Jr, T. H. *J. Chem. Phys.* **1989**, *90*, 1007–1023.

- [183] (a) Jensen, F. J. *Chem. Phys.* **2001**, *115*, 9113–9125; (b) Jensen, F. J. *Chem. Phys.* **2002**, *116*, 3502.
- [184] Hall, G. G. *P. Roy. Soc. Lon. A Mat.* **1951**, *205*, 541–552.
- [185] Roothaan, C. *Rev. Mod. Phys* **1951**, *23*, 69–89.
- [186] Møller, C.; Plesser, M. S. *Phys. Rev.* **1934**, *46*, 618–622.
- [187] Hirata, S.; Bartlett, R. J. *Chem. Phys. Lett.* **2000**, *321*, 216–224.
- [188] Cremer, D. *WIREs Comput. Mol. Sci.* **2011**, *1*, 509–530.
- [189] Bartlett, R. J. *WIREs Comput. Mol. Sci.* **2012**, *2*, 126–138.
- [190] Crawford, T. D.; Schaefer, H. F., III In *Reviews in Computational Chemistry, Volume 14*; Lipkowitz, K. B., Boyd, D. B., Eds.; John Wiley & Sons: Hoboken, NJ, 2000; pp 33–136.
- [191] Bartlett, R.; Musiał, M. *Rev. Mod. Phys* **2007**, *79*, 291–352.
- [192] Hohenberg, P.; Kohn, W. *Phys. Rev.* **1964**, *136*, B864–B871.
- [193] Kohn, W.; Sham, L. J. *Phys. Rev.* **1965**, *140*, A1133–A1138.
- [194] Perdew, J. P.; Schmidt, K. *AIP Conference Proceedings* **2001**, *577*, 1–20.
- [195] Korth, M.; Grimme, S. J. *Chem. Theory Comput* **2009**, *5*, 993–1003.
- [196] Becke, A. D. *Phys. Rev. A* **1988**, *38*, 3098–3100.
- [197] Lee, C.; Yang, W.; Parr, R. G. *Phys. Rev. B* **1988**, *37*, 785–789.
- [198] Perdew, J. P.; Burke, K.; Ernzerhof, M. *Phys. Rev. Lett.* **1996**, *77*, 3865–3868.
- [199] Perdew, J. P.; Burke, K.; Ernzerhof, M. *Phys. Rev. Lett.* **1997**, *78*, 1396.
- [200] (a) Van Voorhis, T.; Scuseria, G. E. *J. Chem. Phys.* **1998**, *109*, 400–410; (b) Van Voorhis, T.; Scuseria, G. E. *J. Chem. Phys.* **2008**, *129*, 219901.
- [201] Zhao, Y.; Truhlar, D. G. *Theor. Chem. Acc.* **2008**, *120*, 215–241.
- [202] Tao, J.; Perdew, J.; Staroverov, V.; Scuseria, G. *Phys. Rev. Lett.* **2003**, *91*, 146401.
- [203] Levy, M. *Phys. Rev. A* **1991**, *43*, 4637–4646.
- [204] Levy, M.; Perdew, J. P. *Phys. Rev. A* **1985**, *32*, 2010–2021.
- [205] Ruzsinszky, A.; Perdew, J. P. *Computational and Theoretical Chemistry* **2011**, *963*, 2–6.

- [206] Vosko, S. H.; Wilk, L.; Nusair, M. *Can. J. Phys.* **1980**, *58*, 1200–1211.
- [207] Becke, A. D. *J. Chem. Phys.* **1993**, *98*, 5648–5652.
- [208] Boese, A. D.; Martin, J. M. L. *J. Chem. Phys.* **2004**, *121*, 3405–3416.
- [209] Staroverov, V. N.; Scuseria, G. E.; Tao, J.; Perdew, J. P. *J. Chem. Phys.* **2003**, *119*, 12129–12137.
- [210] Grimme, S. *J. Chem. Phys.* **2006**, *124*, 034108.
- [211] Zhang, Y.; Xu, X.; Goddard III, W. A. *PNAS* **2009**, *106*, 4963–4968.
- [212] Kozuch, S.; Martin, J. M. L. *Phys. Chem. Chem. Phys.* **2011**, *13*, 20104–20107.
- [213] Ruzsinszky, A.; Perdew, J. P.; Csonka, G. I. *J. Chem. Theory Comput* **2010**, *6*, 127–134.
- [214] Goerigk, L.; Grimme, S. *Phys. Chem. Chem. Phys.* **2011**, *13*, 6670–6688.
- [215] Goerigk, L.; Grimme, S. *J. Chem. Theory Comput* **2011**, *7*, 291–309.
- [216] Jensen, F. *J. Chem. Theory Comput* **2010**, *6*, 2726–2735.
- [217] Lee, D.; Furche, F.; Burke, K. *J. Phys. Chem. Lett.* **2010**, *1*, 2124–2129.
- [218] Perdew, J. P.; Zunger, A. *Phys. Rev. B* **1981**, *23*, 5048–5079.
- [219] Klüpfel, S.; Klüpfel, P.; Jónsson, H. *J. Chem. Phys.* **2012**, *137*, 124102.
- [220] Papas, B. N.; Schaefer, H. F. *J. Mol. Struc-Theochem* **2006**, *768*, 175–181.
- [221] Grimme, S.; Antony, J.; Ehrlich, S.; Krieg, H. *J. Chem. Phys.* **2010**, *132*, 154104.
- [222] Grimme, S.; Ehrlich, S.; Goerigk, L. *J. Comput. Chem.* **2011**, *32*, 1456–1465.
- [223] Cramer, C. J. *Essentials of Computational Chemistry: Theories and Models, second edition*, 2nd ed.; Wiley, 2004.
- [224] Zhao, Y.; Truhlar, D. G. *Acc. Chem. Res.* **2008**, *41*, 157–167.
- [225] Parr, R. G.; Donnelly, R. A.; Levy, M.; Palke, W. E. *J. Chem. Phys.* **1978**, *68*, 3801–3807.
- [226] Parr, R. G.; Pearson, R. G. *J. Am. Chem. Soc.* **1983**, *105*, 7512–7516.
- [227] Pearson, R. G. *J. Mol. Struc-Theochem* **1992**, *255*, 261–270.
- [228] Parr, R. G.; Yang, W. *J. Am. Chem. Soc.* **1984**, *106*, 4049–4050.

- [229] Ayers, P. W.; Parr, R. G. *J. Am. Chem. Soc.* **2000**, *122*, 2010–2018.
- [230] Geerlings, P.; De Proft, F.; Langenaeker, W. *Chem. Rev.* **2003**, *103*, 1793–1874.
- [231] Pearson, R. G. *J. Chem. Sci.* **2005**, *117*, 369–377.
- [232] Feller, D. *J. Chem. Phys.* **1993**, *98*, 7059–7071.
- [233] Feller, D. *J. Chem. Phys.* **1992**, *96*, 6104–6114.
- [234] Halkier, A.; Helgaker, T.; Jørgensen, P.; Klopper, W.; Olsen, J. *Chem. Phys. Lett.* **1999**, *302*, 437–446.
- [235] Peterson, K. A.; Woon, D. E.; Dunning Jr, T. H. *J. Chem. Phys.* **1994**, *100*, 7410–7415.
- [236] Helgaker, T.; Klopper, W.; Koch, H.; Noga, J. *J. Chem. Phys.* **1997**, *106*, 9639–9646.
- [237] Feller, D.; Peterson, K. A.; Grant Hill, J. *J. Chem. Phys.* **2011**, *135*, 044102.
- [238] Curtiss, L. A.; Redfern, P. C.; Raghavachari, K. *WIREs Comput. Mol. Sci.* **2011**, *1*, 810–825.
- [239] Curtiss, L. A.; Raghavachari, K.; Redfern, P. C.; Pople, J. A. *J. Chem. Phys.* **2000**, *112*, 7374–7383.
- [240] Curtiss, L.; Raghavachari, K.; Redfern, P. *J. Chem. Phys.* **1998**, *109*, 7764–7776.
- [241] Curtiss, L. A.; Redfern, P. C.; Raghavachari, K. *J. Chem. Phys.* **2007**, *126*, 084108.
- [242] Curtiss, L. A.; Redfern, P. C.; Raghavachari, K. *J. Chem. Phys.* **2007**, *127*, 124105.
- [243] Pitoňák, M.; Janowski, T.; Neogrady, P.; Pulay, P.; Hobza, P. *J. Chem. Theory Comput* **2009**, *5*, 1761–1766.
- [244] Bader, R. F. W. *Atoms in Molecules: A Quantum Theory*; International Series of Monographs on Chemistry; Oxford University Press: New York, 1990.
- [245] Bader, R. F. W. *J. Phys. Chem. A* **2007**, *111*, 7966–7972.
- [246] Henkelman, G.; Arnaldsson, A.; Jónsson, H. *Comp. Mater. Sci.* **2006**, *36*, 354–360.
- [247] Sanville, E.; Kenny, S. D.; Smith, R.; Henkelman, G. *J. Comput. Chem.* **2007**, *28*, 899–908.

- [248] Tang, W.; Sanville, E.; Henkelman, G. *J. Phys.: Condens. Matter* **2009**, *21*, 084204.
- [249] Pulay, P. In *Applications of Electronic Structure Theory*; Schaefer, H. F., III, Ed.; Springer US, 1977; pp 153–185.
- [250] Schlegel, H. B. *Theor. Chem. Acc.* **2000**, *103*, 0294–0296.
- [251] Pulay, P. *WIREs Comput. Mol. Sci.* **2013**, DOI: 10.1002/wcms.1171.
- [252] Schlegel, H. B. *WIREs Comput. Mol. Sci.* **2011**, *1*, 790–809.
- [253] Ochterski, J. W. *Thermochemistry in Gaussian*. 2000.
- [254] Bühl, M.; van Mourik, T. *WIREs Comput. Mol. Sci.* **2011**, *1*, 634–647.
- [255] Frisch, M. J. et al. *Gaussian 09 Revision A.02*
- [256] SECIL. <http://www.chalmers.se/en/departments/ap/research/cmp/software/Pages/default.aspx>.
- [257] Angenendt, K.; Johansson, P. *J. Phys. Chem. C* **2010**, *114*, 20577–20582.
- [258] Bera, P.; Sattelmeyer, K.; Saunders, M.; Schaefer, H., III; Schleyer, P. J. *Phys. Chem. A* **2006**, *110*, 4287–4290.
- [259] Johansson, P.; Jacobsson, P. *Solid State Ionics* **2006**, *177*, 2691–2697.
- [260] Ufimtsev, I. S.; Martínez, T. J. *J. Chem. Theory Comput* **2009**, *5*, 2619–2628.
- [261] Kästner, J.; Carr, J. M.; Keal, T. W.; Thiel, W.; Wander, A.; Sherwood, P. J. *Phys. Chem. A* **2009**, *113*, 11856–11865.
- [262] Kita, F.; Kawakami, A.; Sonoda, T.; Kobayashi, H. In *New Sealed Rechargeable Batteries and Super Capacitors, The Electrochemical Society Proceedings Series*; Barnett, B. M., Dowgiallo, E., Halpert, G., Matsuda, Y., Takehara, Z., Eds.; Electrochemical Society: Pennington, NJ, 1993; p 321.
- [263] Koopmans, T. *Physica* **1934**, *1*, 104–113.
- [264] Ue, M.; Murakami, A.; Nakamura, S. *J. Electrochem. Soc.* **2002**, *149*, A1572–A1577.
- [265] Perdew, J. P.; Parr, R. G.; Levy, M.; Balduz Jr, J. *Phys. Rev. Lett.* **1982**, *49*, 1691–1694.
- [266] Kleinman, L. *Phys. Rev. B* **1997**, *56*, 12042–12045.
- [267] Stowasser, R.; Hoffmann, R. *J. Am. Chem. Soc.* **1999**, *121*, 3414–3420.

- [268] Xue, Z.-M.; Chen, C.-H. *Electrochim. Acta* **2004**, *49*, 5167–5175.
- [269] Ossola, F.; Pistoia, G.; Seeber, R.; Ugo, P. *Electrochim. Acta* **1988**, *33*, 47–50.
- [270] Xu, K.; Ding, S. P.; Jow, T. R. *J. Electrochem. Soc.* **1999**, *146*, 4172–4178.
- [271] Vollmer, J. M.; Curtiss, L. A.; Vissers, D. R.; Amine, K. *J. Electrochem. Soc.* **2004**, *151*, A178–A183.
- [272] Trasatti, S. *Pure & Appl. Chem.* **1986**, *58*, 955–966.
- [273] Scheers, J.; Johansson, P.; Szczeciński, P.; Wieczorek, W.; Armand, M.; Jacobsson, P. *J. Power Sources* **2010**, *195*, 6081–6087.
- [274] Bartlett, R. J. *Int. J. Mol. Sci* **2002**, *3*, 579–603.
- [275] O'boyle, N. M.; Morley, C.; Hutchison, G. R. *Chem. Cent. J.* **2008**, *2*, 5.
- [276] O'boyle, N. M.; Banck, M.; James, C. A.; Morley, C.; Vandermeersch, T.; Hutchison, G. R. *J. Cheminform.* **2011**, *3*, 33.
- [277] Jónsson, E.; Johansson, P. *Phys. Chem. Chem. Phys.* **2012**, *14*, 10774–10779.
- [278] Scheers, J.; Pitawala, J.; Thebault, F.; Kim, J.-K.; Ahn, J.-H.; Matic, A.; Johansson, P.; Jacobsson, P. *Phys. Chem. Chem. Phys.* **2011**, *13*, 14953–14959.
- [279] Zhou, Z.-B.; Takeda, M.; Fujii, T.; Ue, M. *J. Electrochem. Soc.* **2005**, *152*, A351–A356.
- [280] Foropoulos Jr, J.; DesMarteau, D. D. *Inorg. Chem.* **1984**, *23*, 3720–3723.
- [281] Gnanaraj, J. S.; Levi, M. D.; Gofer, Y.; Aurbach, D.; Schmidt, M. *J. Electrochem. Soc.* **2003**, *150*, A445–A454.
- [282] Koch, V.; Dominey, L.; Nanjundiah, C.; Ondrechen, M. J. *J. Electrochem. Soc.* **1996**, *143*, 798–803.
- [283] Kita, F.; Sakata, H.; Sinomoto, S.; Kawakami, A.; Kamizori, H.; Sonoda, T.; Nagashima, H.; Nie, J.; Pavlenko, N. V.; Yagupolskii, Y. L. *J. Power Sources* **2000**, *90*, 27–32.
- [284] Xu, W.; Shusterman, A. J.; Videa, M.; Velikov, V.; Marzke, R.; Angell, C. A. *J. Electrochem. Soc.* **2003**, *150*, E74–E80.
- [285] Sasaki, Y.; Handa, M.; Kurashima, K.; Tonuma, T.; Usami, K. *J. Electrochem. Soc.* **2001**, *138*, A999–A1003.
- [286] Zhang, S. S. *J. Power Sources* **2007**, *163*, 713–718.

- [287] Nanbu, N.; Tsuchiya, K.; Shibasaki, T.; Sasaki, Y. *Electrochem. Solid-State Lett.* **2002**, *5*, A202–A205.
- [288] Eberwein, M.; Schmid, A.; Schmidt, M.; Zabel, M.; Burgemeister, T.; Barthel, J.; Kunz, W.; Gores, H. J. *J. Electrochem. Soc.* **2003**, *150*, A994–A999.
- [289] Niedzicki, L.; Grugeon, S.; Laruelle, S.; Judeinstein, P.; Bukowska, M.; Prejzner, J.; Szczeciński, P.; Wieczorek, W.; Armand, M. *J. Power Sources* **2011**, *196*, 8696–8700.

Appendices

A Recombinator program

This is a short high-level description of the Recombinator program used in Paper VI. It is written in Python and utilises the OpenBabel library^{275,276} for force field optimisation. The code is split into modules:

Atom.py A utility class that represents individual atoms. It also gives information on whether additional bonds can be created, *i.e.* checks whether the atoms has fewer than the maximum allowed bonds, *e.g.* 1 for H, 4 for C, *etc.*. It also checks what kind of bonding is possible, from the number of electrons on the atom available for bonding, and how many more electrons can be added.

Molecule.py A class that in essence is a list of atoms with the bonding information. Each molecule has a method that take a bond number as an argument, and returns a list of paired molecular fragments, which have the all of the possible electron distributions. This means that for H₂, three pairs of fragments will be generated; H⁺ and H⁻, H· and H·, and H⁻ and H⁺.

Exporter.py A simple way to take a molecule object and export as a Gaussian (or any other implemented program) input file.

OB_interface.py An interface with the OpenBabel library, used for simple optimisation. All bonding information needs to be manually input, as there can be issues with the automated bonding done by OpenBabel, which is written for more sensible structures.

Recombinator.py Takes two fragments and tries to combine them by first locating where their bonds have been broken. Second, it attempts to add a bond between the atoms that had bonds prior, this is done by using functions of the atoms to check on compatibility between the two fragments. Thus a lewis acid can bond with a lewis base, and a

radical with a radical. Third, if bonding was successful, the resulting new molecule is optimised with OpenBabel.

runner.py A program that uses the power of the various classes to decompose molecules, as defined in the inputted configuration file and recombine the fragments. It is also capable of pruning out structures which are not novel, as the program will generate a large number of such structures.

B Anions

Through my studies I ran across a number of different anions that have been proposed or used for LIB/SIB electrolytes. Here is a list, which aims to be comprehensive, of the anions reported in the literature. For values to be included in the table, they must have been published (or in the case of Na-salts of the pseudo-delocalized, not destined for publication).

Structures are given for relevant anions, excluding trivial/well known structures.

Properties

ΔE_d Calculated ion pair dissociation energy, both values for Li^+ , $\Delta E_{d \text{ Li}}$, and Na^+ , $\Delta E_{d \text{ Na}}$. B3LYP/6-311+G* (if no superscript), kJ mol^{-1} . Starred values are new and cannot be found in any of the papers in this thesis or references. Superscripts used for the ΔE_d values have the following meaning:

- a: G4MP2
- b: M06-2X/6-311+G*
- c: BMK/6-311+G*
- d: TPSSh/6-311+G*

ΔE_v Calculated vertical ionisation potential, given in V vs. Li^+/Li^0 . Values that were not calculated with at the VSXC/6-311+G* level of theory are marked.

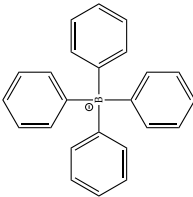
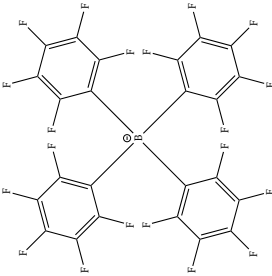
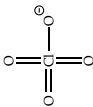
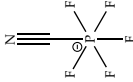
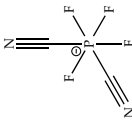
IP_K The IP calculation of Kaymaksiz *et al.*,⁹² given in V vs. Li^+/Li^0 .

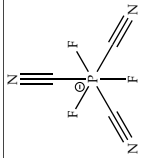
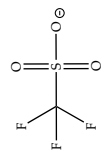
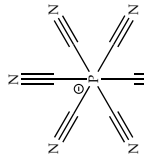
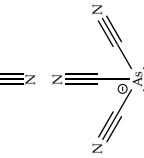
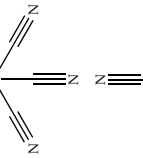
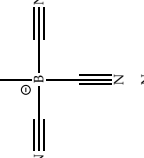
ΔE_{ox} Measured oxidation potential, if not given vs. Li^+/Li^0 , then it is noted in the table.

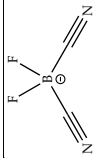
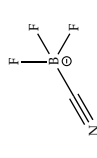
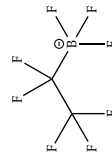
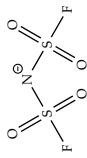
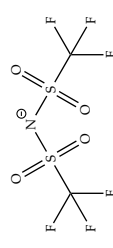
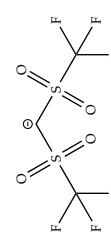
ΔE_{red} Measured reduction potential

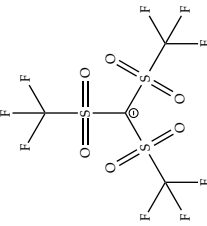
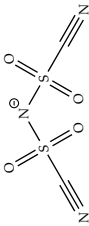
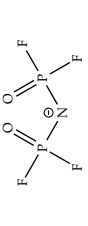
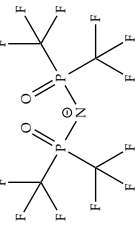
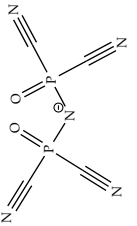
Anion	Name	Structure	Property	Ref.
SIMPLE ANIONS				
BH_4^-	tetrahydroborate		$\Delta E_{d, Li} = 654.4; \Delta E_{d, Na} = 552.1$	81,277
Br^-	bromine		$\Delta E_{d, Li} = 612.5; \Delta E_{d, Na} = 529.2$	81,277
BrO_3^-	bromate		$\Delta E_{d, Li} = 615.8; \Delta E_{d, Na} = 551.0$	81,277
CH_3COO^-	acetate		$\Delta E_{d, Li} = 721; \Delta E_{d, Na} = 613.2$	81,277
Cl^-	chlorine		$\Delta E_{d, Li} = 720.6; \Delta E_{d, Na} = 613.2$	81,277
F^-	fluorine		$\Delta E_{d, Li} = 643.7; \Delta E_{d, Na} = 550.6$	81,277
HCO_2^-	formate		$\Delta E_{d, Li} = 773.5; \Delta E_{d, Na} = 644.9$	81,277
HF_2^-			$\Delta E_{d, Li} = 704.3; \Delta E_{d, Na} = 602.3$	81,277
HS^-	thiol		$\Delta E_{d, Li} = 682.7; \Delta E_{d, Na} = 578.6$	81,277
NCO^-	isocyanate		$\Delta E_{d, Li} = 641.6; \Delta E_{d, Na} = 557.9$	81,277
NO_3^-	nitrate		$\Delta E_{d, Li} = 653.0; \Delta E_{d, Na} = 546.2$	81,277

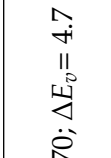
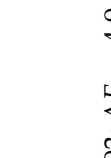
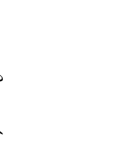
Anion	Name	Structure	Property	Ref.
SCN ⁻	thiocyanate		ΔE_d Li ⁺ = 648.3; ΔE_d Na ⁺ = 545.5	81,277
TRADITIONAL WEAKLY COORDINATING ANIONS				
AsF ₆ ⁻	hexafluoroarsenate		ΔE_d Li ⁺ = 558.6; ΔE_d Na ⁺ = 479.8; ΔE_v = 6.05; E_{ox} = 6.8, 8.6	64,76,81, 277
SbF ₆ ⁻	hexafluorostibate		E_{ox} = 7.1, 8.8	76
B(CH ₃) ₄ ⁻	tetramethylborate		ΔE_d Li ⁺ = 612.6; ΔE_d Na ⁺ = 491.4; ΔE_v = 2.21; E_{ox} = 2.9	76,81,112, 277
B(CH ₃)(C ₂ H ₅) ₃ ⁻	methyltriethylborate		E_{ox} = 5.2	76
B(C ₂ H ₅) ₄ ⁻	tetraethylborate		E_{ox} = 5.1	76
BF ₄ ⁻	tetrafluoroborate		ΔE_d Li ⁺ = 601.7; ΔE_d Na ⁺ = 515.9; ΔE_v = 5.22; E_{ox} = 6.6, 8.3	64,76,81, 277

Anion	Name	Structure	Property	Ref.
$B(Ph)_4^-$	tetraphenylborate, $B(C_6H_5)_4^-$		$\Delta E_{d, Li} = 554.1$; $\Delta E_{d, Na} = 482.3$; $\Delta E_v = 3.15$; $E_{ox} = 4.0$, 4.3	76,81,112, 277
$B(C_6F_5)_4^-$	tetrakis(perfluorophenyl)- borate		$E_{ox} = 5.2$	76
ClO_4^-	perchlorate		$\Delta E_{d, Li} = 593.8$; $\Delta E_{d, Na} = 498.6$; $E_{ox} = 6.1$, 7.0	76,277
PF_6^-	hexafluorophosphate		$\Delta E_{d, Li} = 567.0$; $\Delta E_{d, Na} = 485.6$; $\Delta E_v = 5.65$; $E_{ox} = 6.8$, 8.4	64,76,81, 277
$PF_5(CN)^-$	cyanopentafluorophosphate			85
$PF_4(CN)_2^-$	dicyanotetrafluorophosphate			85

Anion	Name	Structure	Property	Ref.
$\text{PF}_3(\text{CN})_3^-$	tricyanotrifluorophosphate		85	
Tf	triflate, CF_3SO_3^-		$\Delta E_{d Li} = 594.5; \Delta E_{d Na} = 502.7; \Delta E_v = 3.60; E_{ox} = 6.0, 7.0$	64,76,277
$\text{P}(\text{CN})_6^-$	hexacyanophosphate		$\Delta E_{d Li} = 452; \Delta E_v = 6.24$	112
$\text{As}(\text{CN})_6^-$	hexacyanoarsenate		$\Delta E_{d Li} = 455; \Delta E_v = 6.18$	112
Bison	$\text{B}(\text{CN})_4^-$		$\Delta E_{d Li} = 479; \Delta E_v = 5.65; E_{ox} \geq 4.0$	112,278
$\text{B}(\text{CN})_3\text{F}^-$	tricyanofluoroborate		$\Delta E_{d Li} = 506; \Delta E_v = 5.43$	112

Anion	Name	Structure	Property	Ref.
$B(CN)_2F_2^-$	dicyanodifluoroborate		$\Delta E_{d Li} = 536; \Delta E_v = 5.16$	112
$B(CN)F_3^-$	cyanotrifluoroborate		$\Delta E_{d Li} = 557; \Delta E_v = 5.34$	112
FAB	pentafluoroethyltri- fluoroborate, $B(C_2F_5)F_3^-$		$E_{ox} \geq 4$	279
IMIDE ANIONS				
FSI	bis(fluorosulfonyl) imide, $(FSO_2)N^-$		$\Delta E_{d Li} = 580.4; \Delta E_{d Na} = 485.6; \Delta E_v = 4.6; E_{ox} = 5.6$	83,85,277
TFSI	bis(trifluoromethanesulfonyl) imide, $(CF_3SO_2)N^-$		$\Delta E_{d Li} = 591.7; \Delta E_{d Na} = 490.5; \Delta E_v = 4.52; E_{ox} = 6.3, 7.1$	64,76,81, 277,280
PFSI	bis(pentafluoroethanesulfonyl) imide, $(C_2F_5SO_2)_2N^-$		$\Delta E_{d Li} = 582.8; \Delta E_{d Na} = 483.6; E_{ox} \geq 5$	277,281
TFSM	bis(trifluoromethanesulfonyl) methide, $(CF_3SO_2)_2CH^-$		$\Delta E_{d Li} = 599.6; \Delta E_{d Na} = 499.8$	277

Anion	Name	Structure	Property	Ref.
TriTFSM	tris(trifluoromethanesulfonyl) methide, $(\text{CF}_3\text{SO}_2)_3\text{C}^-$		$\Delta E_{d, Li} = 560.2$; $\Delta E_{d, Na} = 461.5$; $\Delta E_v = 4.57$; $E_{ox} = 5.65$	64,277,282
CSI	bis(cyanosulfonyl) imide, $(\text{NCSO}_2)_2\text{N}^-$		$\Delta E_{d, Li} = 547$; $\Delta E_v = 5.1$	85
FPI	bis(difluorophosphoryl) imide, $(\text{F}_2\text{PO})\text{N}^-$		$\Delta E_{d, Li} = 641$; $\Delta E_v = 4.2$	85
TFPI	bis(bis(trifluoromethyl)phosphoryl) imide, $((\text{CF}_3)_2\text{PO})\text{N}^-$		$\Delta E_{d, Li} = 615$; $\Delta E_v = 4.7$	85
CPI	bis(dicyanophosphoryl) imide, $((\text{CN})_2\text{PO})\text{N}^-$		$\Delta E_{d, Li} = 570$; $\Delta E_v = 5.2$	85
FTFSI	(fluorosulfonyl)(trifluoromethylsulfonyl) imide, $(\text{CF}_3\text{SO}_2)(\text{FSO}_2)\text{N}^-$		$\Delta E_{d, Li} = 584$; $\Delta E_v = 4.4$	85
CFSI	(cyanosulfonyl)(fluorosulfonyl) imide, $(\text{NCSO}_2)(\text{FSO}_2)\text{N}^-$		$\Delta E_{d, Li} = 563$; $\Delta E_v = 4.8$	85

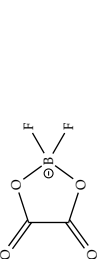
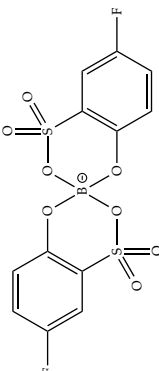
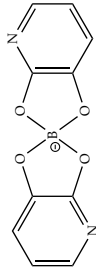
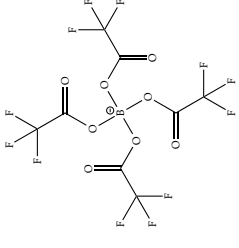
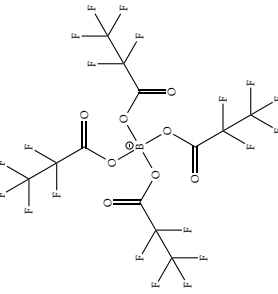
Anion	Name	Structure	Property	Ref.
CTFSI	(cyanosulfonyl)(trifluoromethyl)sulfonyl imide, (NCSO ₂)(F ₃ CSO ₂)N ⁻		$\Delta E_{d Li} = 570$; $\Delta E_v = 4.7$	85
FTFPI	(bis(trifluoromethyl)phosphoryl)(difluorophosphoryl) imide, ((CF ₃) ₂ PO)(F ₂ PO)N ⁻		$\Delta E_{d Li} = 627$; $\Delta E_v = 4.4$	85
CFPI	(dicyanophosphoryl)(difluorophosphoryl) imide, ((NC) ₂ PO)(F ₂ PO)N ⁻		$\Delta E_{d Li} = 604$; $\Delta E_v = 4.9$	85
CTFPI	(bis(trifluoromethyl)phosphoryl)(dicyanophosphoryl) imide, ((NC) ₂ PO)((CF ₃) ₂ PO)N ⁻		$\Delta E_{d Li} = 593$; $\Delta E_v = 4.9$	85
DMSI	cyclo-difluoromethane-1,1-bis(sulfonyl) imide, (SO ₂ CF ₂ SO ₂)N ⁻		$E_{ox} = 5.01$	86
HPSI	cyclo-hexafluoropropane-1,1-bis(sulfonyl) imide, (SO ₂ (CF ₂) ₃ SO ₂)N ⁻		$E_{ox} = 4.62$	86

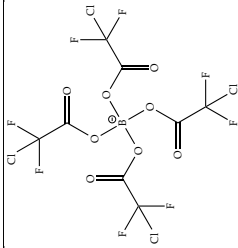
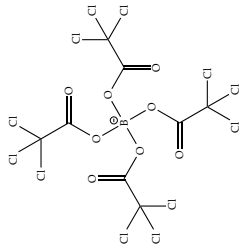
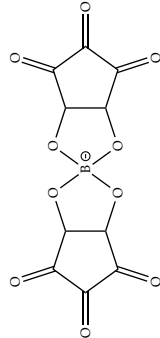
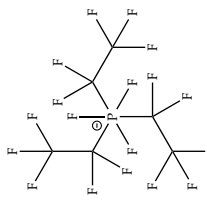
Anion	Name	Structure	Property	Ref.
Kita-1	bis((2,2,2-trifluoroethoxy)sulfonyl)imide, (CF ₃ CH ₂ OSO ₂) ₂ N ⁻		$E_{ox} = 5.4$	283
Kita-2	tetrafluoropropoxy-sulfonyl) imide, (HCF ₂ CF ₂ CH ₂ OSO ₂) ₂ N ⁻		$E_{ox} = 5.5$	283
Kita-3	pentafluoropropoxy-sulfonyl) imide, (CF ₃ CF ₂ CH ₂ OSO ₂) ₂ N ⁻		$E_{ox} = 5.6$	283
Kita-4	bis(((1,1,1,3,3,3-hexafluoropropan-2-yl)oxy)sulfonyl) imide, ((CF ₃) ₂ CHOSO ₂) ₂ N ⁻		$E_{ox} = 5.8$	283
BORON BASED ANIONS				
BBB	bis[1,2-benzene-diolato(2-)-O,O'] borate, B(C ₆ H ₄ O ₂) ₂ ⁻		$\Delta E_{d Li} = 579.5; \Delta E_{d Na} = 484.2; \Delta E_v = 1.79; E_{ox} = 3.6$	64,87,277
FBBB	bis[3-fluoro-1,2-benzenediolato(2-)-O,O'] borate, B(C ₆ H ₃ O ₂ F) ₂ ⁻		$E_{ox} = 4.7$	79,88

Anion	Name	Structure	Property	Ref.
4F-BBB	bis[tetrafluoro-1,2-benzenediolato(2-)-O,O'] borate, $B(C_6F_4O_2)_2^-$		$\Delta E_{d, Li} = 497.4$; $\Delta E_{d, Na} = 415.5$; $\Delta E_v = 2.79$; $E_{ox} = 4.0$	64,79,277
BBPB	bis[2,2'-biphenyldiolato(2-)-O,O'] borate, $B(C_{12}H_8O_2)_2^-$		$\Delta E_{d, Li} = 592.7$; $\Delta E_{d, Na} = 500.4$; $E_{ox} = 4.1$	89,277
BMB	bis(malonato) borate, $B(C_3O_4H_2)_2^-$		$\Delta E_{d, Li} = 524.5$; $\Delta E_{d, Na} = 458.5$	277,284
BNB	bis[2,3-naphthalenediolato(2-)-O,O'] borate, $B(C_{10}H_6O_2)_2^-$		$\Delta E_{d, Li} = 550.5$; $\Delta E_{d, Na} = 456.0$; $\Delta E_v = 1.43$; $E_{ox} = 3.7$	64,79,277
BOB	bis(oxolato)borate, $B(C_2O_4)_2^-$		$\Delta E_{d, Li} = 520.6$; $\Delta E_{d, Na} = 433.5$; $\Delta E_v = 4.05$; $IP_K = 5.98$	64,92,277, 284
BFFPB	bis(perfluoropinacolato)orthoborate, $B(C_6O_2F_{12})_2^-$		$\Delta E_{d, Li} = 533.0$; $\Delta E_{d, Na} = 453.8$; $E_{ox} \geq 4.5$	93,277,284

Anion	Name	Structure	Property	Ref.
BSB	bis[salicylato(2-)] borate, $B(C_7H_4O_3)_2^-$		$\Delta E_{d, Li} = 592.5$; $\Delta E_{d, Na} = 506.7$; $E_{ox} = >4.5$, 4.46; $IP_K = 4.46$	89,92,277
MOB	(malonatooxalato) borate, $B(C_3O_4H_2)(C_2O_4)^-$		$\Delta E_{d, Li} = 535.4$; $\Delta E_{d, Na} = 445.5$; $E_{ox} = 4.3$	96,277
SOB	salicylatooxalato borate, $B(C_2O_4)(C_7H_4O_3)^-$		$E_{ox} = 4.51, 4.75$; $IP_K = 4.75$	92
BBrSB	bis(5-bromosalicylato) borate, $B(C_7O_3H_3Br)_2^-$		$E_{ox} = 4.47, 4.70$; $IP_K = 4.47$	92
BCISB	$B(C_7O_3H_3Cl)_2^-$		$E_{ox} \geq 4.5$; $IP_K = 4.57$	92

Anion	Name	Structure	Property	Ref.
BCI2SB	bis(3,5-dichloro-salicylato) borate, bis(5-chlorosalicylato) borate, $B(C_7O_3H_2Cl_2)_2^-$		$E_{ox} = 4.55, 4.80; IP_K = 4.62$	92,285
BCI3SB	bis(2,3,5-trichloro-salicylato) borate, $B(C_7O_3HCl_3)_2^-$		$E_{ox} \approx 4.5$	285
BFSB	bis(5-fluorosalicylato) borate, $B(C_7O_3H_3F)_2^-$		$E_{ox} = 4.4, 4.65; IP_K = 4.49$	92
BMSB	bis(3-methylsalicylato) borate, $B(C_8H_6O_3)_2^-$		$E_{ox} = 4.36; IP_K = 4.33$	92,285

Anion	Name	Structure	Property	Ref.
DFOB	difluoro(oxolato) borate $B(C_2O_4)F_2^-$		$E_{ox} \geq 4.2$	65,98,286
BFBSB	bis(5-fluoro-2-olato-1-benzenesulfonato(2-)-O,O') borate, $B(C_6H_3FO_4S)_2^-$		$E_{ox} = 4.6$	90
BPB	bis(5-fluoro-2-olato-1-benzenesulfonato(2-)-O,O') borate, $B(C_5H_3NO_2)_2^-$		$E_{ox} = 3.95$	91
TFAB	tetrakis(trifluoroacetoxy) borate, $B(CO_2CF_3)_4^-$		$E_{ox} \geq 4.5$	95
PFPB	tetrakis(pentafluoropropoxy) borate, $B(CO_2C_2F_5)_4^-$		$E_{ox} \geq 4.5$	95

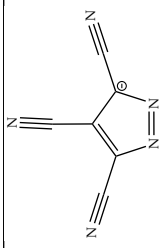
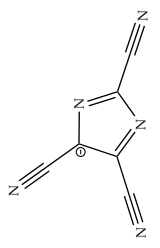
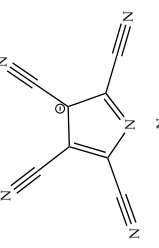
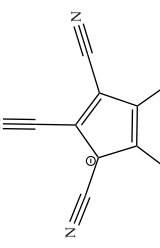
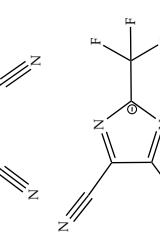
Anion	Name	Structure	Property	Ref.
CDFAB	tetrakis(chlorodifluoro- acetoxy) borate, $B(\text{CO}_2\text{CClF}_2)_4^-$		$E_{\text{ox}} \geq 4.5$	95
TCAB	tetrakis(trichloro- acetoxy) borate, $B(\text{CO}_2\text{CCl}_3)_4^-$		$E_{\text{ox}} \geq 4.5$	95
BCB	bis(croconato) borate, $B(\text{C}_5\text{O}_5)_2^-$		$E_{\text{ox}} = 5.5$	111
FAP	fluoroalkyl- phosphate $\text{PF}_3(\text{C}_2\text{F}_5)_3^-$		$\Delta E_{d, Li} = 531.8; \Delta E_{d, Na} = 446.1; E_{\text{ox}} \geq 4$	77,277,281

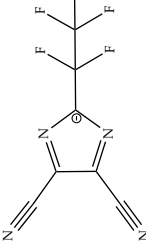
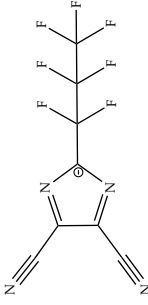
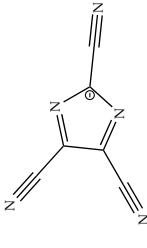
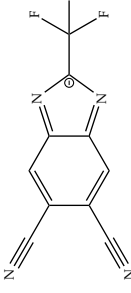
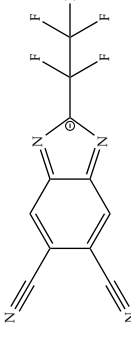
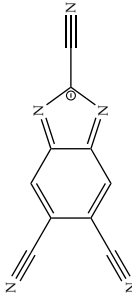
PHOSPHORUS ANIONS

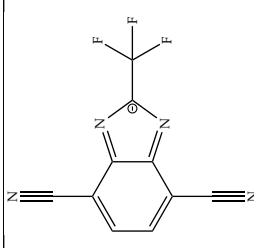
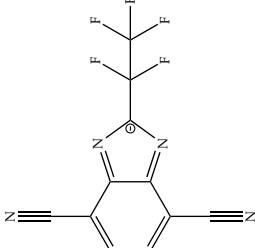
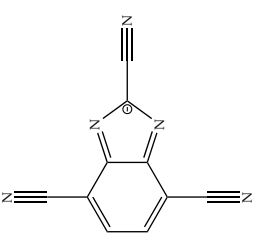
Anion	Name	Structure	Property	Ref.
P1	tris[1,2-benzenediolato(2-)-O,O'] phosphate, $P(C_6H_4O_2)_3^-$		$\Delta E_{d, Li} = 604.5$; $\Delta E_{d, Na} = 506.0$; $E_{ox} = 3.7$	101,277
P2	tris[3-fluoro-1,2-benzenediolato(2-)-O,O'] phosphate, $P(C_6H_3FO_2)_3^-$		$\Delta E_{d, Li} = 594.0$; $\Delta E_{d, Na} = 505.9$; $E_{ox} = 4.1, 3.95$	277,287,288
P3	tris[3,4,5,6-tetrafluoro-1,2-benzenediolato(2-)-O,O'] phosphate, $P(C_6F_4O_2)_3^-$		$\Delta E_{d, Li} = 507.0$; $\Delta E_{d, Na} = 426.2$; $E_{ox} = 4.5$	277,288
$PF_3(CF_3)_3^-$	$PF_3(CF_3)_3^-$		$\Delta E_{d, Li} = 544.4$; $\Delta E_{d, Na} = 463.4$; $E_{ox} = 5.1$	99,277
$PF_4(CF_3)_2^-$	$PF_4(CF_3)_2^-$		$\Delta E_{d, Li} = 557.6$; $\Delta E_{d, Na} = 472.4$; $E_{ox} = 6.2$	99,277

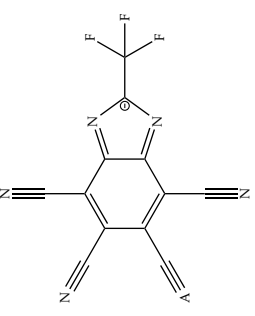
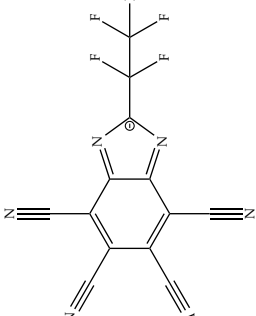
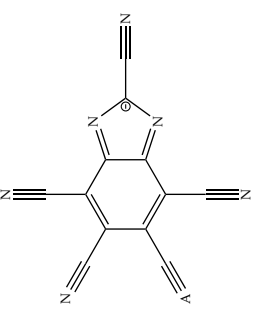
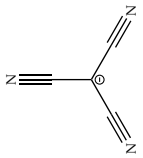
Anion	Name	Structure	Property	Ref.
PF_5CF_3^-	PF_5CF_3^-		$\Delta E_{d, Li} = 554.0$; $\Delta E_{d, Na} = 477.7$; $E_{ox} = 6.2$	99,277
TOP	$\text{P}(\text{C}_2\text{O}_4)^-$		$\Delta E_{d, Li} = 482.6$; $\Delta E_{d, Na} = 397.6$; $E_{ox} = 5.5$	100,277
TFOP	$\text{PF}_4(\text{C}_2\text{O}_4)^-$			102
HETEROCYCLIC RING-BASED ANIONS				
$\text{Im}(\text{BF}_3)_2^-$	bis(trifluoroborane)-imidazolate, $\text{N}_2\text{C}_2\text{H}_3(\text{BF}_3)_2^-$		$\Delta E_{d, Li} = 495.6$; $\Delta E_{d, Na} = 446.9$; $\Delta E_{ox} = 4.58$; $\Delta E_{ox} = 4.85^{zz}$	64,108,277
2-MeIm(BF_3) $_2^-$	bis(trifluoroborane)-2-methylimidazolate, $\text{C}_4\text{H}_5\text{N}_2(\text{BF}_3)_2^-$			109
4-MeIm(BF_3) $_2^-$	bis(trifluoroborane)-4-methylimidazolate, $\text{C}_4\text{H}_5\text{N}_2(\text{BF}_3)_2^-$			109

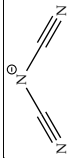
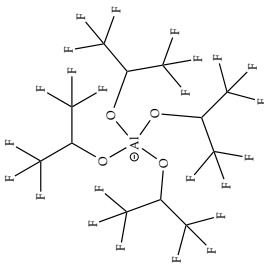
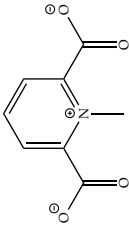
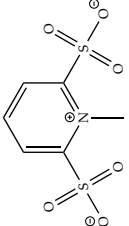
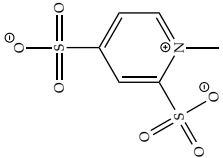
Anion	Name	Structure	Property	Ref.
2- <i>i</i> PrIm(BF ₃) ₂ ⁻	bis(trifluoroborane)-2-isopropylimidazololate, C ₆ H ₉ N ₂ (BF ₃) ₂ ⁻			109
BenzIm(BF ₃) ₂ ⁻	bis(trifluoroborane)-benzimidazololate C ₇ H ₅ N ₂ (BF ₃) ₂ ⁻			109
N(CH ₃) ₂ (BF ₃) ₂ ⁻	Bis(trifluoroborane)-dimethylamide, N(CH ₃) ₂ (BF ₃) ₂ ⁻			109
N ₅ ⁻	N ₅ ⁻		$\Delta E_{d Li} = 576.4; \Delta E_{d Na} = 491.7$	155,277
N ₅ C ₂ ⁻	N ₅ C ₂ ⁻		$\Delta E_{d Li} = 558.9; \Delta E_{d Na} = 474.0$	155,277
TADC (or DCTA)	4,5-dicyano-1,2,3-triazolate, N ₅ C ₄ ⁻		$\Delta E_{d Li} = 540.5; \Delta E_{d Na} = 454.8; \Delta E_v = 3.72$	64,155,277
N ₅ C _{4b} ⁻	3,5-dicyano-1,2,4-triazolate, N ₅ C ₄ ⁻		$\Delta E_{d Li} = 542.9; \Delta E_{d Na} = 456.1$	155,277

Anion	Name	Structure	Property	Ref.
PATC	3,4,5-tricyano-3H-pyrazol-3-ide, $N_5C_6^-$		$\Delta E_{d Li} = 523.9$; $\Delta E_{d Na} = 437.3$	155,277
$N_5C_6^-$	2,4,5-tricyano-4H-imidazol-4-ide, $N_5C_6^-$		$\Delta E_{d Li} = 493.0$; $\Delta E_{d Na} = 419.8$; $\Delta E_v = 3.5$	155,273,277
$N_5C_8^-$	2,3,4,5-tetracyano-3H-pyrrol-3-ide		$\Delta E_{d Li} = 479.4$; $\Delta E_{d Na} = 407.3$	155,277
PNCP	1,2,3,4,5-pentacyano-cyclopentadienide, $N_5C_{10}^-$		$\Delta E_{d Li} = 466.3$; $\Delta E_{d Na} = 395.5$; $\Delta E_v = 3.97$	112,155,277
TDI	4,5-dicyano-2-(trifluoromethyl)imidazolide, $C_5N_4CF_3^-$		$\Delta E_{d Li} = 516$; $\Delta E_v = 3.5$; $E_{ox} \geq 4.3$	105,106, 156,273,289

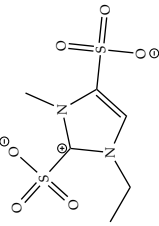
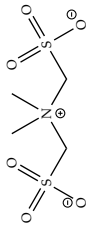
Anion	Name	Structure	Property	Ref.
PDI	4,5-dicyano-2-(pentafluoroethyl)imidazolide, $C_5N_4C_2F_5^-$		$\Delta E_{dLi} = 513$; $\Delta E_v = 3.6$; $E_{ox} \geq 4.3$	105,106, 156,273,289
HDI	4,5-dicyano-2-(n-heptafluoropropyl)imidazolide, $C_5N_4C_3F_7^-$		$E_{ox} \geq 4.5$	106,107
CDI	2,4,5-tricyanoimidazolide, $C_5N_4CN^-$		$\Delta E_{dLi} = 493$; $\Delta E_v = 3.5$;	273
TDB ₅₆	5,6-dicyano-2-trifluoromethyl-benzimidazolide, $C_9H_2N_4CF_3^-$		$\Delta E_{dLi} = 516$; $\Delta E_v = 3.4$	273
PDB ₅₆	5,6-dicyano-2-pentafluoroethylbenzimidazolide, $C_9H_2N_4C_2F_5^-$		$\Delta E_{dLi} = 514$; $\Delta E_v = 3.5$	273
CDB ₅₆	2,5,6-tricyano-benzimidazolide, $C_9H_2N_4CN^-$		$\Delta E_{dLi} = 488$; $\Delta E_v = 3.4$	273

Anion	Name	Structure	Property	Ref.
TDB ₄₇	4,7-dicyano-2-trifluoromethylbenzimidazolide, C ₉ H ₂ N ₄ CF ₃ ⁻		$\Delta E_{dLi} = 556; \Delta E_v = 3.3$	273
PDB ₄₇	4,7-dicyano-2-pentafluoroethylbenzimidazolide, C ₉ H ₂ N ₄ C ₂ F ₅ ⁻		$\Delta E_{dLi} = 560; \Delta E_v = 3.4$	273
CDB ₄₇	2,4,7-tricyanobenzimidazolide, C ₉ H ₂ N ₄ CN ⁻		$\Delta E_{dLi} = 543; \Delta E_v = 3.5$	273

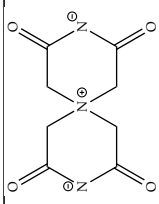
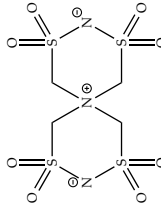
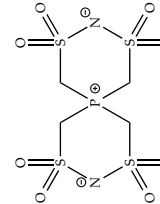
Anion	Name	Structure	Property	Ref.
TTB	4,5,6,7-tetracyano-2-trifluoromethylbenzimidazolide, $C_{11}N_6CF_3^-$		$\Delta E_{d Li} = 497; \Delta E_v = 4.2$	273
PTB	4,5,6,7-tetracyano-2-pentafluoroethylbenzimidazolide, $C_{11}N_6C_2F_5^-$		$\Delta E_{d Li} = 502; \Delta E_v = 4.2$	273
CTB	2,4,5,6,7-pentacyano-benzimidazolide, $C_{11}N_6CN^-$		$\Delta E_{d Li} = 484; \Delta E_v = 4.3$	273
	OTHER ANIONS			
$C(CN)_3^-$			$\Delta E_{d Li} = 501.2; \Delta E_{d Na} = 433.0$	277

Anion	Name	Structure	Property	Ref.
$\text{N}(\text{CN})_2^-$	$\text{N}(\text{CN})_2^-$		$\Delta E_{d, Li} = 558.6$; $\Delta E_{d, Na} = 474.2$	277
$\text{Al}(\text{HFIP})_4^-$	$\text{Al}(\text{C}_3\text{HF}_6\text{O}_4)^-$		$\Delta E_{d, Li} = 533.2$; $\Delta E_{d, Na} = 451.0$	110,277
PSEUDO-DELOCALIZED ANIONS				
Pyridine based				
1,3C2MePy	1,3-dicarboxylate-2-methyl-pyridine, $(\text{CO}_2)_2\text{CH}_3\text{C}_5\text{H}_3\text{N}^-$		$\Delta E_{d, Li} = 597.5$, $\Delta E_{d, Na} = 501.0^*$, $\Delta E_v = 2.90$	82
1,3S2MePy	1,3-disulfonate-2-methyl-pyridine, $(\text{SO}_3)_2\text{CH}_3\text{C}_5\text{H}_3\text{N}^-$		$\Delta E_{d, Li} = 567.4$, $\Delta E_{d, Na} = 475.9^*$, $\Delta E_v = 3.65$	82
2,4S1MePy	2,4-disulfonate-1-methyl-pyridine, $(\text{SO}_3)_2\text{CH}_3\text{C}_5\text{H}_3\text{N}^-$		$\Delta E_{d, Li} = 580.7$, $\Delta E_{d, Na} = 490.9^*$, $\Delta E_v = 3.47$	82

Anion	Name	Structure	Property	Ref.
1,3S5MePy	1,3-disulfonate-5-methyl-pyridine, (SO ₃) ₂ CH ₃ C ₅ H ₃ N ⁻		$\Delta E_{dLi} = 596.7$, $\Delta E_{dNa} = 505.7^*$, $\Delta E_v = 3.27$	82
1,4S2MePy	1,4-disulfonate-2-methyl-pyridine, (SO ₃) ₂ CH ₃ C ₅ H ₃ N ⁻		$\Delta E_{dLi} = 542.0$, $\Delta E_{dNa} = 452.1^*$, $\Delta E_v = 3.57$	82
1,3MeS2MePy	1,3-dimethylsulfonate-2-methyl-pyridine, (CH ₂ SO ₃) ₂ CH ₃ C ₅ H ₃ N ⁻		$\Delta E_{dLi} = 704.8$, $\Delta E_{dNa} = 603.8^*$, $\Delta E_v = 3.29$	82
1,3OIm	1,3-dioxo-imidazole, O ₂ C ₃ H ₃ N	Imidazolium based 	$\Delta E_{dLi} = 598.4$, $\Delta E_{dNa} = 492.3^*$, $\Delta E_v = 0.74$	82
1,3SIm	1,3-disulfonate-imidazole, (SO ₃) ₂ C ₃ H ₃ N ⁻		$\Delta E_{dLi} = 661.0$, $\Delta E_{dNa} = 459.5^*$, $\Delta E_v = 4.12$	82
1,3MeSIm	1,3-dimethylsulfonate-imidazole, (CH ₂ SO ₃) ₂ C ₃ H ₃ N ⁻		$\Delta E_{dLi} = 659.5$, $\Delta E_{dNa} = 565.1^*$, $\Delta E_v = 3.57$	82

Anion	Name	Structure	Property	Ref.
1Et2,4S3Melm	1-ethyl-2,4-disulfonate-3-methyl-imidazole, $C_3H_8(SO_3)_2C_3HN^-$		$\Delta E_{dLi} = 558.6$, $\Delta E_{dNa} = 469.8^*$, $\Delta E_v = 3.57$	82
DSDMA	disulfonate-dimethyl-amine, $(SO_3)_2(CH_3)_2N^-$	Ammonium based 	$\Delta E_{dLi} = 635.8$, $\Delta E_{dNa} = 540.5^*$, $\Delta E_v = 3.82$	82
MeSDMA	dimethylsulfonate-dimethyl-amine, $(CH_2SO_3)_2(CH_3)_2N^-$		$\Delta E_{dLi} = 553.5$, $\Delta E_{dNa} = 521.3^*$, $\Delta E_v = 3.58$	82
EtSDMA	diethylsulfonate-dimethyl-amine, $((CH_2)_2SO_3)_2(CH_3)_2N^-$		$\Delta E_{dLi} = 661.0$, $\Delta E_{dNa} = 554.6^*$, $\Delta E_v = 3.28$	82
PrSDMA	dipropylsulfonate-dimethyl-amine, $((CH_2)_3SO_3)_2(CH_3)_2N^-$		$\Delta E_{dLi} = 659.5$, $\Delta E_{dNa} = 561.2^*$, $\Delta E_v = 3.13$	82
BuSDMA	dibutylsulfonate-dimethyl-amine, $((CH_2)_4SO_3)_2(CH_3)_2N^-$		$\Delta E_{dLi} = 788.7$, $\Delta E_{dNa} = 682.7^*$, $\Delta E_v = 2.63$	82

Spiros

Anion	Name	Structure	Property	Ref.
SCA	spiro-carboxyl-amine, (-CH ₂ CONCOCH ₂ -) ₂ N ⁻		$\Delta E_{dLi} = 604.9$, $\Delta E_{dNa} = 501.1^*$, $\Delta E_v = 3.32$	82
SSA	spiro-sulfone-amine, (-CH ₂ SO ₂ NSO ₂ CH ₂ -) ₂ N ⁻		$\Delta E_{dLi} = 546.9$, $\Delta E_{dNa} = 450.3^*$, $\Delta E_v = 4.27$	82
SSP	spiro-sulfone-phosphine, (-CH ₂ SO ₂ NSO ₂ CH ₂ -) ₂ P ⁻		$\Delta E_{dLi} = 562.9$, $\Delta E_{dNa} = 467.9^*$, $\Delta E_v = 4.45$	82

